neel.cnrs.fr

Highlights 2014

NÉEL institut

Editorial

The Institut NEEL was founded in 2007 by amalgamating four of the CNRS's Grenoble laboratories and bringing in several other Grenoble teams. Since then, our ambition has been to rank as one of the best laboratories in the world in our specific fields of scientific research, principally basic research in condensed-matter physics, enriched by interdisciplinary activities at the interfaces with chemistry, engineering and biology. It is always a challenge to measure the quality and impact of research activity. Numbers exist but have to be interpreted carefully. However, at the scale of the Institut NEEL, the main indicator of our success and visibility is the publication of about 400 scientific papers per year in highly ranked basic research journals and the high numbers of citations these articles attract.

The present issue (No. 8) of the Institut NEEL's "Highlights" magazine contains 19 short articles specially written to describe particularly important technical or scientific advances made over the last one or two years. Given the size of our laboratory, this is far from being an exhaustive list. A much more complete overview of our activities can be found at our website www.neel.cnrs.fr, which details the research work of each of our 17 research teams and describes our six major research fields

- Magnetism and spintronics
- Photonics, plasmonics and non-linear optics
- Correlated systems, quantum fluids and superconductivity
- Quantum, molecular and wide bandgap electronics
- Materials: synthesis, structure and functions
- Instrumentation

and our transverse actions Theory, Energy, Very large Experimental Systems, Chemistry and Biophysics. Our website also provides pdf versions of all previous issues of our "Highlights" magazine.

Besides our vocation to develop cutting-edge research in the above fields, our missions also include the dissemination of scientific knowledge to society. This involves creating effective contacts with the general public and communicating research news to diverse audiences. "Highlights" magazine contributes to this task by targeting readers with a certain scientific background (students, engineers, professionals...). For a wider audience, we have recently created a visitors' centre at Institut NEEL, the "Physiquarium" : It offers a pedagogical presentation of our laboratory's research subjects (both historical aspects and an introduction to our current projects) and allows visitors to perform simple experiments.

Following on from our contributions to the International Year of Crystallography in 2014, the Institut NEEL will be involved in the International Year of Light and Light-based Technologies (IYL 2015) proclaimed by UNESCO for 2015. Given the extent of our research in optics and photonics, predicted to be two key enabling technologies of the future, Institut NEEL staff are preparing exhibitions and other events to be organized in the framework of IYL-2015 in Grenoble and elsewhere in France.

Alain SCHUHL
Director of Institut NEEL
Grenoble, France

Contents

Scanning gate microscopy on a quantum point contact 3

The quantum diffusion of muons in the spin ice $Dy_2Ti_2O_7$ 4

Diamond Schottky diodes for high power electronics 5

Table-top Helium 3 cryostat 6

Tunable light emission from a boron nitride nanotube device 7

Low temperature damping in a nano-electro-mechanical device 8

Tunable superconductivity in an array of metal dots decorating graphene 9

Vortex creep in type II superconductors : when vortices cross walls 10

Fibered nano-optical tweezers for micro- and nano-particle trapping 11

Unravelling structure and magnetism in strongly correlated systems 12

New mm-wave instrument ("NIKA") opens for astronomers 13

At the interface between ab initio calculations and correlated models 14

Mesoscopic spin glasses 15

Superconductivity Dome around a Quantum Critical Point 16

Bloch-point Domain Walls in cylindrical magnetic nanowires 17

Evaporation of helium in a porous material 18

Strain couples a nano-mechanical oscillator and a quantum emitter 19

Activation mechanism in the hydrogen storage material MgH_2 20

DIRECTOR OF PUBLICATION
Alain SCHUHL

EDITORS
Signe SEIDELIN, Ronald COX

LAYOUT - PRODUCTION
Elodie BERNARD
Nathalie BOURGEAT-LAMI
Florence FERNANDEZ

COVER
SYNTHESE ECA

PRINTING
Press Vercors

Date of publication: 2014

Scanning gate microscopy on a quantum point contact

The electrical conductance through a nanometer-scale constriction in a plane of electrons exhibits quantized values that reveal the quantum properties of the electrons. In addition, a puzzling anomaly appears below the first quantum step in the graph of conductance versus gate voltage and remains the subject of intensive experimental and theoretical research. Especially, this effect could be the manifestation of a localized electronic state induced by the Coulomb interactions between electrons. We have applied a scanning gate technique on such a device to elucidate this intriguing phenomenon.

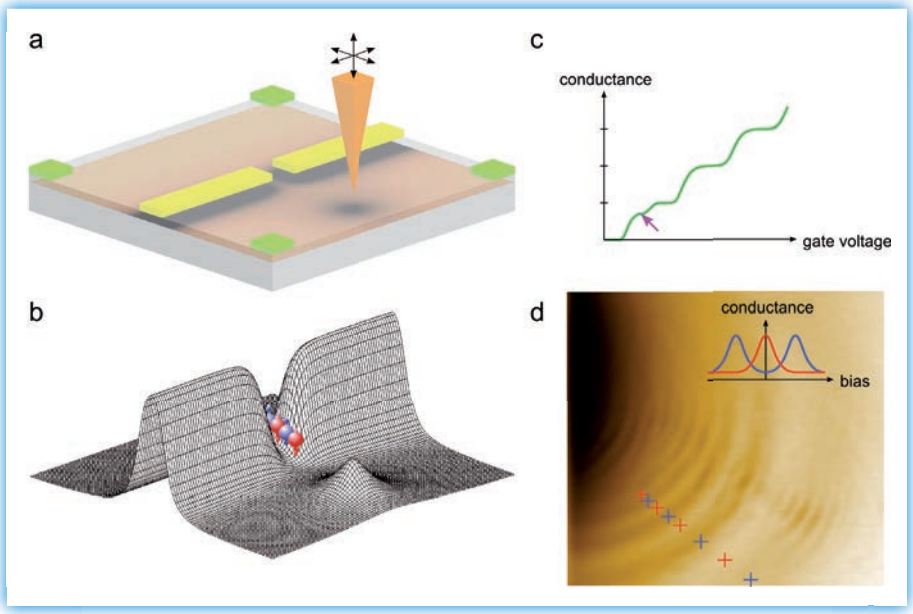

Fig. 1 : (a) Schematic of the quantum point contact defined by a metallic split-gate (yellow) on a two-dimensional electron gas (brown) connected with four contacts (green). In our work, a sharp metallic tip (orange) acts as a movable gate to do scanning gate microscopy.

(b) Simulation of the electrostatic potential induced by the split-gate and by the tip, also showing a chain of electrons localized in the channel (blue electrons spin up, red electrons spin down).

(c) Channel conductance versus split-gate voltage, showing quantized conductance plateaux and the "0.7 anomaly" (arrow).

(d) Scanning gate image (700 x 750 nm) of the conductance versus tip position (the split-gate is on the left). The image reveals concentric rings induced by the periodic splittings (in blue) of the zero-bias conductance peak (in red) shown schematically in the inset.

Quantum point contacts are very simple electronic devices made by the deposition of a metallic split-gate on the surface of a semiconductor heterostructure containing a plane of electrons. Applying a negative voltage on this split-gate creates a narrow channel connecting two large electron reservoirs (see Fig. 1a). Due to the transverse quantization of their quantum mechanical wave functions, electrons propagate through the channel in discrete modes, like photons in optical waveguides. The number of available modes is determined by the channel width and controlled by the voltage on the split-gate. Each mode carries current with a quantized conductance equal to $2e^2/h$. Thus, the electrical characteristic of a quantum point contact at low temperature is a nice staircase with equally spaced plateaux (see Fig. 1c).

In addition to this ideal behavior, an anomaly is frequently observed at a conductance value around 0.7 x $2e^2/h$ (see arrow in Fig. 1c). This phenomenon cannot be explained correctly by existing theories. It is probably related to the strong Coulomb interactions between electrons in the constriction, where their density is very low and their kinetic energy very small. In such extreme conditions, theory predicts the formation of a strongly correlated state, named the "Wigner crystal", where the electron charges are spatially ordered and the electron spins are coupled antiferromagnetically (see Fig. 1b). Moreover, the observation of a narrow conductance peak at zero bias (zero potential difference between the reservoirs) indicates the existence of a localized spin in the channel, which is coupled to the reservoirs via the "Kondo effect" (many-body screening of a degenerate spin state by conduction electrons).

To establish whether such a localized and correlated electron state exists and to investigate its structure, we use the sharp metallic tip of a scanning-probe microscope. We apply a negative voltage on the tip, bring it close to the sample surface, and scan it around the constriction (Fig. 1a). This scanning gate technique offers a very flexible way to finely tune the electrostatic potential of the point contact (Fig. 1b) in conjunction with the fixed split-gates. These experiments were done in collaboration with researchers at the Université Catholique de Louvain (Belgium) whose apparatus can reach very low temperatures (40 mK).

Moving the tip around the constriction while the conductance is near 0.7 x $2e^2/h$, we discovered that the conductance anomaly oscillates periodically when the tip approaches the constriction. The oscillations appear as concentric rings in the scan images (see Fig. 1d). At the same time, the conductance peak at zero bias splits periodically into two peaks at finite bias (see inset of Fig. 1d). This behaviour corresponds to alternating equilibrium and non-equilibrium Kondo effects. It indicates that the localized state switches periodically between half-integer and integer spin states. This result is consistent with the presence of a one-dimensional Wigner crystal in the channel, containing an increasing number of localized electrons as the scanning gate progressively modifies the potential shape of the constriction.

One can predict that ways will be found in the future to observe these localized charges directly, for example by electrostatic force microscopy.

CONTACT

Hermann SELLIER
hermann.sellier@neel.cnrs.fr

Ph.D student
Boris BRUN

FURTHER READING

Wigner and Kondo physics in quantum point contacts revealed by scanning gate microscopy
B. Brun et al.,
Nature Communications 5, 4290 (2014)

The quantum diffusion of muons in the spin ice $Dy_2Ti_2O_7$

Among the magnetic probes available for studying condensed matter, muon Spin Relaxation (mu-SR) occupies an important place. This technique is highly sensitive to local magnetic fields and can probe spin fluctuations over time scales from roughly 10^{-5} to 10^{-12} seconds. However, the interpretation of mu-SR spectra is not always straightforward owing to the multitude of different interactions that the muons experience in matter. While mu-SR spectra are well understood in many compounds, including some magnetic oxides, their interpretation for the "magnetically frustrated", pyrochlore-lattice compounds remains challenging.

The mu-SR spectrum of the archetypal spin ice Dysprosium Titanate ($Dy_2Ti_2O_7$ or "DTO") appears however to have revealed an unexpected spin dynamics (i.e. large fluctuations of the spins). The muon data suggest that the Dy atom spins fluctuate at a constant time scale of the order of 10^{-6} s from the lowest temperatures yet investigated (a few mK) up to about 7K. This phenomenon has often been called the "persistent spin dynamics" but is problematic for two reasons. First, other magnetic probes do not reveal such a fast, temperature-independent dynamics. For example, recent A.C. susceptibility measurements indicate spin fluctuation rates up to 10 orders of magnitude slower at the lowest temperatures than those suggested by mu-SR studies. Secondly, the theory of spin-ices is now relatively well-understood and it is quite difficult to justify such fast spin dynamics theoretically. In theory, the spins should freeze almost completely below about 0.5 K in DTO.

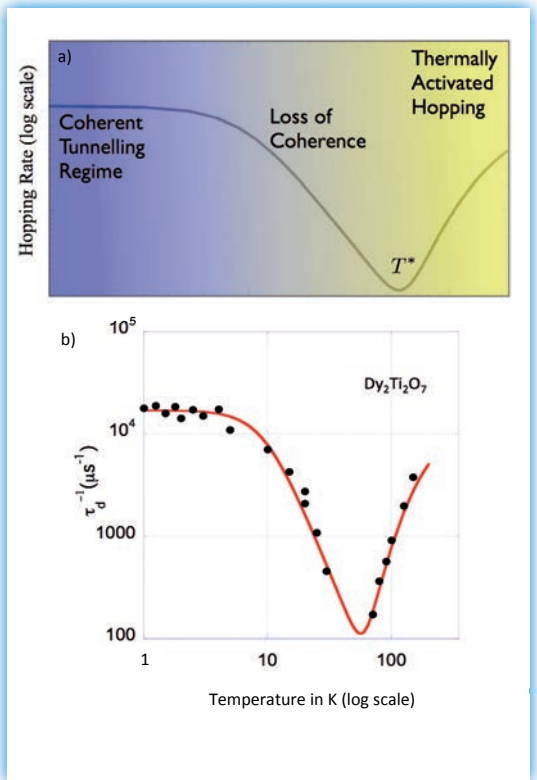

The crystal structure of a spin-ice consists of atomic spins (the magnetic Disprosium ions in the case of DTO) disposed at the corners of tetrahedra. The strong Ising magnetic anisotropy imposes that the spins at the corners are directed either towards the centre of the tetrahedron or in the opposite direction. That leads to a "frustrated" nature of the magnetism (no given spin can couple anti-parallel with its three neighbours simultaneously) and to the so-called "ice-rule", or "two-in, two-out" rule : Two spins must point towards the centre, and two in the opposite direction.

A standard experiment with muons consists of sending positively charged, *spin-polarized* muons (charge e+, spin ½) along a given direction in the studied sample. What is measured is then the depolarization of the muon spins with time. The relaxation rate thus obtained gives us information about the magnetic fluctuations that the muons have felt during their 2.2 microsecond lifetime.

Clearly, there are two main possibilities. The first one is that the muons have become localized in the sample. The only sources of magnetic fluctuations then come from the temporal fluctuations of the spin structure itself. The muons would act here as local probes and it is under this hypothesis that the existence of a "persistent spin dynamics" in DTO has been claimed.

The second possibility is the reverse one : the spins in the structure are assumed frozen at low temperature and the muons are moving. We have adopted the latter hypothesis. Owing to its charge and large mass (207 times that of the electron), a muon interacts very strongly with the phonons of a dielectric such as DTO. That results in a composite particle called a polaron, a muon "dressed" with the crystal's phonons. This object moves as a whole, and calculations show that there are three regimes of diffusion as function of the temperature (see Fig. 1(a)). In the diffusion scenario, the muon spin relaxation rate is proportional to its diffusion time. Our interpretation faithfully reproduces the experimental data of S. R. Dunsiger et al (PRL 2011) over a very wide temperature range (see Fig. 1(b)) and there is so far no other competitive theory.

Our work gives the first scenario that can rule out the "persistent spin dynamics" hypothesis for systems like DTO. To go further, we have also measured mu-SR in an equivalent but non-magnetic compound: $Y_2Ti_2O_7$. Here, the muons are found to be sensitive to the spin nuclei and to magnetic defects like Ti^{3+} ions.

Fig. 1: In (a), the motion of a polaron is characterized by three regimes. At low temperatures, the diffusion rate (or hopping rate) is almost temperature independent. This indicates coherent quantum tunnelling of the particle. At higher temperatures, interaction with phonons progressively destroys the coherent motion up to a temperature T, where the diffusion rate is minimum. Above T*, an incoherent and thermally activated regime takes place.*
In (b): muon spin relaxation times (data points) extracted from the mu-Spin Relaxation experiment on $Dy_2Ti_2O_7$ (Dunsiger et al 2011) compared with our theoretical curve for polaronic muon diffusion.

CONTACT

Pascal QUEMERAIS
pascal.quemerais@neel.cnrs.fr

FURTHER READING

Muon diffusion and electronic magnetism in $Y_2Ti_2O_7$
J.A. Rodriguez, A. Yaouanc, B. Barbara, E. Pomjakushina, P. Quémerais and Z. Salman
Phys. Rev. B 87, 184427 (2014)

Possible quantum diffusion of polaronic muons in $DY_2Ti_2O_7$ spin ice
P. Quémerais, P. McClarty and R. Moessner
Phys. Rev. Lett. 109, 127601 (2012)

Diamond Schottky diodes for high power electronics

Diamond has a relatively wide bandgap but it can be made into a semiconductor, or even a metal, by doping it with impurity atoms. Semiconducting diamond layers, grown epitaxially on diamond substrates, have outstanding electrical and thermal properties in view of high power applications. Diamond high power devices are now being intensively investigated. In particular, Schottky diodes based on a metal/diamond junction appear very promising: high breakdown voltages up to 10 kV have been achieved, though unfortunately associated with a high forward resistance. In recent advances, we have made significant progress in minimizing the forward resistance and obtained unprecedented Figures of Merit for diamond Scottky junction devices.

Diodes for high power electronics are required to pass ever higher currents in the forward direction and to sustain ever higher voltages in the reverse direction. Such diodes will be used for example in high power switching in DC/DC convertors to supply electric motors. Driven by recent environmental protection requirements and cost reduction imperatives, new diodes are needed. They will have to sustain up to 3.3 kV reverse voltage while allowing 1 ampère forward current.

The Schottky potential barrier at a metal-semiconductor contact is ideal for fast switching, and for low voltage drop in the forward regime. To fabricate Schottky diodes from diamond, we deposit a metal electrode on an oxygen terminated, p-type (boron doped), semiconducting diamond epilayer. That layer was grown on top of a metallic (p^{++}) diamond epilayer which acts as the back contact. The pseudo-vertical structure realized is illustrated in Fig. 1.

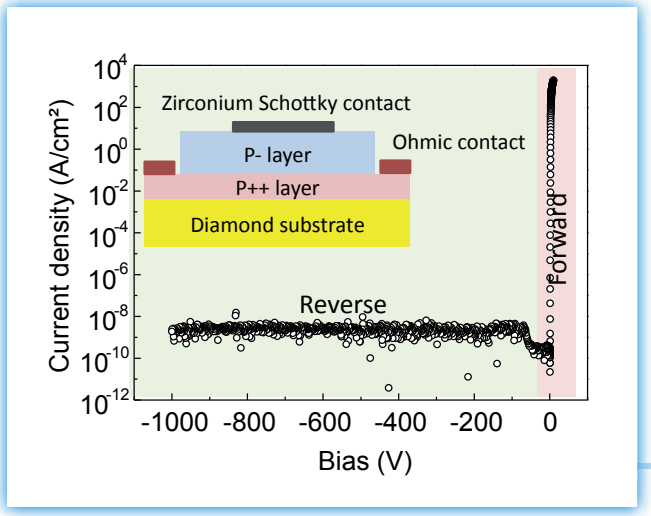

Fig. 1: Typical current-voltage characteristics at 300 K for one zirconium/p-type diamond Schottky diode deposited on a diamond substrate. The data show the high reverse voltage, and the high forward currents achieved.

To ensure good rectifying behavior, we have focused our work on various metal-diamond interfaces and have demonstrated that the readily oxidised metal zirconium (Zr) is an excellent candidate to make efficient Schottky barriers. Fig. 1 shows the current-voltage (I–V) characteristic at room temperature for one of our Zr/diamond Schottky diodes. Zirconium Schottky contacts exhibited an extremely good rectification behaviour characterized by a high current density of 10^3 A/cm² (at +6 V), and a reverse current density smaller than 10^{-8} A/cm² up to our maximum test voltage *Vmax* = -1000 V. Given the semiconductor layer thickness of 1.3 µm in our vertical structure, the reverse field reached was 7.7 MV/cm.

An important "Figure of Merit" used to evaluate high power Schottky diodes is the ratio $Vmax^2/(R_{on}S)$, where R_{on} is the specific forward resistance and S the diode surface. For room temperature Zr/p-diamond we have obtained an unprecedented value of 244 (in units of MW/cm²). This value lies far above the limit for silicon (10 MW/cm²). It is today the largest value reported for diamond Schottky diodes and may be compared to the theoretical value (1000 MW/cm²).

A high resolution Transmission Electron Microscopy study undertaken by colleagues from the University of Cadiz (Spain) showed the presence of an oxide at the Zr/diamond interface (see Fig. 2). This oxide provides strong passivation of interface defects, which no doubt explains the excellent reproducibility of our I–V characteristics. For instance, 83 out of a total of 100 diodes characterized had reverse current below a threshold of 1.3×10^{-9} A/cm².

We have found that annealing our Zr/p-diamond Schottky diodes can reduce significantly the voltage threshold allowing high forward current. This is related to a reduction of the Schottky barrier height, e.g. from 1.88 eV for as-deposited diodes to 1.49 eV for diodes annealed at 350°C. Finally, we have measured a current of 1 A through a square (500x500 µm²) diode. We should mention that several uncertainties affect the barrier height estimates, but Zr/p-diamond diodes annealed at temperatures as high as 450°C displayed a barrier height estimated at 1 eV, and the diode structure remained stable up to 500°C.

The performances reported here for Zr/p-diamond diodes confirm the potential of diamond for high power electronics applications. A French patent was filed in 2013 (ref. 13.53647 "Procédé de fabrication d'une diode Schottky sur un substrat en diamant").

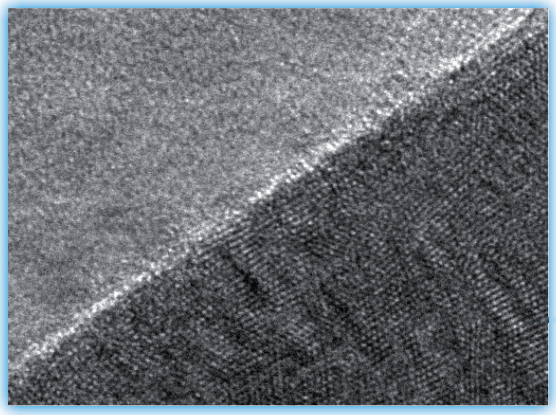

Fig. 2: High resolution Transmission Electron Microscope image of a Zirconium/Diamond interface lying in the [001] lattice plane. The bright atoms correspond to the oxide layer which passivates the interface. Courtesy of José Piñero (Cadiz University).

CONTACT

David EON
david.eon@neel.cnrs.fr

Ph.D student
Aboulaye TRAORE

FURTHER READING

Zr/oxidized diamond interface for high power Schottky diodes.
A.Traore, P. Muret, A. Fiori, D. Eon, E. Gheeraert and J. Pernot
Appl. Phys. Lett. 104, 052105 (2014)

Table-top Helium 3 cryostat

Cryostats that use the rare isotope He^3 as cooling fluid to achieve temperatures below 1 degree K can be very complex to operate. A prototype of a user-friendly, "table-top" Helium 3 cryostat has been designed and built recently at NEEL Institute in order to satisfy a research team's needs for frequent electrical characterization measurements at very low temperature. This cryostat can cool samples down to 300 mK very quickly, in about 3 hours.

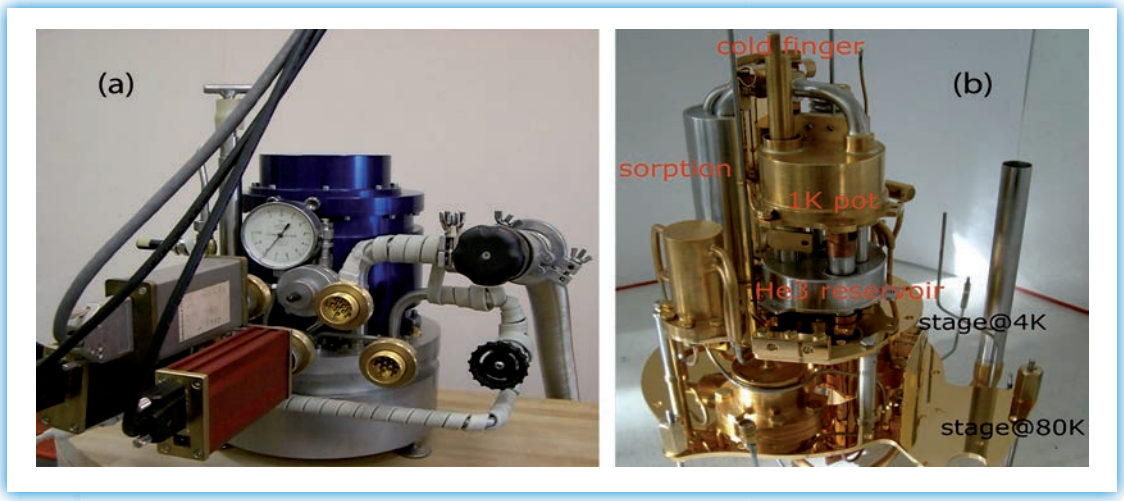

Fig. 1 (a): The table-top Helium 3 cryostat showing the compactness of the system. (b): A photo with the external shell removed. Visible are the 1 K pot, the He^3 reservoir, the sorption system, and the cold finger emerging through the 1 K pot. The sample holder (not shown here) mounts on top of the cold finger. The stages are thermal shields that block the external radiation.

Josephson junctions, two superconductors coupled by a thin insulator barrier, are the building blocks of low temperature superconducting quantum circuits. Their fabrication implies the use of high quality superconductor thin films whose properties must be very well characterized. Especially, the temperature and the width (in deg. K) of the superconducting transition of the films all have to be known. Then, after fabrication in a clean room by techniques such as lithography and etching, the quantum circuits themselves have to be tested at low temperature. A table-top Helium 3 cryostat has been created in order to perform these electrical characterizations quickly.

As shown in Fig. 1(a), this cryostat is very compact and can be placed on a laboratory work table. It is composed of a vacuum chamber (50 cm high and 20 cm diameter) containing two helium circuits interlocked with each other. The first helium circuit is an open circuit containing liquid Helium 4, which flows around the cryostat from the supply reservoir to the helium gas recovery exhaust. The second circuit is a closed Helium 3 circuit, containing a small quantity of this very rare and extremely expensive isotope. As the coldest part of the cryostat is at its top, the sample holder is very accessible, just below the two thermal screens and the cover, which makes loading the sample much easier than in conventional designs where the sample compartment is at the bottom of the cryostat.

The basic principle of a Helium 3 cryostat is to condense He^3 gas to the liquid inside a reservoir by bringing the gas in contact with a pumped Helium 4 reservoir (the "1 K pot", see Fig. 1(b); liquid He^4 can be cooled to about 1 degree K by strong pumping). The temperature inside the Helium 3 reservoir can then be lowered to around 300 mK by reducing the vapour pressure on the liquid He^3. This is achieved with an internal, sorption pumping system (activated charcoal, Fig. 1(b) "sorption"). When all the Helium 3 has been adsorbed (no liquid He^3 left), the charcoal is reheated at 40 K in order to liberate the adsorbed gas. A new condensation cycle can then be initiated.

The sample holder is thermally connected to the Helium 3 reservoir via the cold finger shown in Fig 1(b). This connection allows us to cool the sample down from 1 K to 300 mK. But the initial cooling of the sample holder from 300 K to 4 K requires a thermal connection with the 1 K pot in order to be efficient and rapid. The setting-up of a *thermal switch* allows this connection for temperatures to 4 K. This "switch" is a small closed volume of Helium exchange gas which can be adsorbed using a dedicated small sorption pump. Below 4 K, the He gas is adsorbed and the switch is turned off.

The available cooling power is 100 µW at 390 mK. During the early phase of testing the performance of the cryostat, 300 mK was reached in a time of 3 hours. The lowest temperature achieved was 280 mK. The working time available before the need to regenerate He^3 liquid is several hours. The regeneration phase requires half an hour.

Up to now, two kinds of superconducting thin films have been characterized : thin films of rhenium produced at SIMAP lab (Laboratory for Materials and Processes Science and Engineering, Grenoble) and thin films of niobium evaporated in the Néel Institute's recently upgraded ultra-high vacuum system.

The cryostat was created by Pierre Brosse-Maron according to an idea of Bernard Pannetier and Philippe Gandit.

CONTACTS

Pierre BROSSE-MARON
pierre.brosse-maron@neel.cnrs.fr

Cécile NAUD
cecile.naud@neel.cnrs.fr

Tunable light emission from a boron nitride nanotube device

Scientists have worked hard in the last few decades to grow nanostructures free of defects. The near-perfect atomic arrangements obtained at the nanometre scale have been employed to create new, efficient devices such as light-emitters, transistors and sensors. However, while many applications benefit from using defect-free materials, the presence of certain defects can generate new and fascinating properties. In the study described here, we have shown that the structural defects that exist in Boron Nitride nanotubes can be put to maximum use as a variable wavelength light source. The outcome of this research is a patent for a light-emitting source that can easily be incorporated into current microelectronics technology.

Boron Nitride BN is a promising material in the field of nanotechnology, thanks to its excellent insulating properties, its high mechanical strength, and its two-dimensional crystal structure similar to graphene. And specifically, the properties of hexagonal boron nitride nanotubes, the focus of this research, appear far superior to those of other materials currently being used as light emitters, for example, in applications linked to optical storage (DVD's...) or communications.

Boron nitride is extremely efficient in ultraviolet light emission, one of the best materials currently available. However, boron nitride nanotubes emit light in a very limited range of the ultraviolet spectrum. This means they cannot be used in applications where the emission needs to be produced in a controlled way over a broad range of wavelengths (including in the visible spectrum).

We have found a solution to overcome this limitation, which opens the way to the use of hexagonal BN nanotubes in commercial applications. By means of numerical simulations, we have investigated light emission in BN nanotubes in the presence of defects. We have shown that, by applying an electric field perpendicular to a nanotube containing particular lattice defects (atomic vacancies, carbon impurity atoms), it will be possible to get the nanotubes to emit light across the whole spectrum from the infrared to the far ultraviolet and to control the wavelength in a simple way (see Fig. 1). This easy tuning by an electric field is only to be found with nanotubes. It is related to their cylindrical geometry (they are tubular structures with diameters of order nanometres, lengths of order microns). These predictions of the theory show the way to new devices based on BN nanotubes.

The generic configuration of the proposed device (see Fig. 2) comprises as-grown BN nanotubes deposited on an insulating surface that acts as a dielectric, to enable the application of the gated electric field that tunes the light emission. The configurations is very similar to that of a Field Effect Transistor (FET).

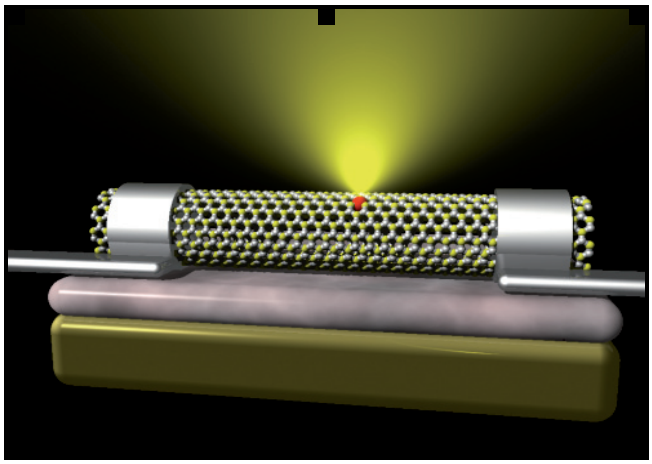

Fig. 2: Schematic set-up for the proposed method of activating an optoelectronic device based on Boron Nitride nanotubes with lattice defects (red dot). The method uses an ambipolar transistor configuration. BN nanotubes are deposited on an insulating surface that acts as a gate dielectric to enable application of the transverse electric field that controls the wavelength of the light emission.

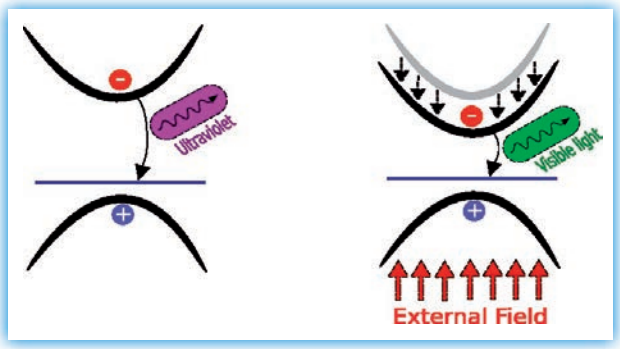

Fig. 1: Simplified band structure diagram for a BN nanotube with and without application of a perpendicular electric field. The electric field shifts the conduction band relative to the defect level (blue line), thus tuning the wavelength of the light emitted when an electron and a hole annihilate at the defect.

CONTACT

Claudio ATTACALITE
claudio.attacalite@neel.cnrs.fr

FURTHER READING

Efficient Gate-tunable light-emitting device made of defective boron nitride nanotubes: from ultraviolet to the visible
C. Attaccalite, L Wirtz, A Marini, A Rubio
Nature Scientific Reports 3, 2698 (2013

Coupling of excitons and defect states in boron-nitride nanostructures
C. Attaccalite, M. Bockstedte, A. Marini, A. Rubio, L. Wirtz
Phys. Rev. B 83 (14), 144115 (2011)

Low temperature damping in a nano-electro-mechanical device

Solid matter can be found in two states depending on the ordering of its atoms : Crystalline solids display a characteristic translational long-range order, whereas amorphous solids lack it. Amorphous materials are of the utmost importance scientifically and technologically. To obtain a fundamental understanding of the nature of these materials, many low temperature experiments have been done that probe dielectric, acoustic, mechanical and thermal properties. These are all macroscopic, bulk properties. To study the nature of amorphous materials at the nanometre scale, Nanometric Electro-Mechanical Systems (NEMSs) can be used. These systems are ideal tools to probe the friction processes occurring in amorphous materials.

Experimental results on amorphous materials are usually discussed in the framework of the well-known Standard Tunnelling Model of Two-Level Systems due to P.M. Anderson and W.A. Phillips. In this model, amorphous materials are assumed to contain "Two Level Systems" (TLSs) whose nature (apart from a few remarkable cases) is essentially unknown. The distribution of the energy splitting between the two levels is assumed to be very broad, and can be modelled by a constant density-of-states *n*. The TLSs are assumed diluted enough to be independent. All properties are then described by two parameters: the density of states *n* and a second parameter *g*, the strength of the coupling to phonons and/or electrons. As concerns the mechanical damping, of interest in our experiments, the attenuation mechanism is thus essentially the energy flow from the mechanical mode to the phonon bath through the Two Level Systems.

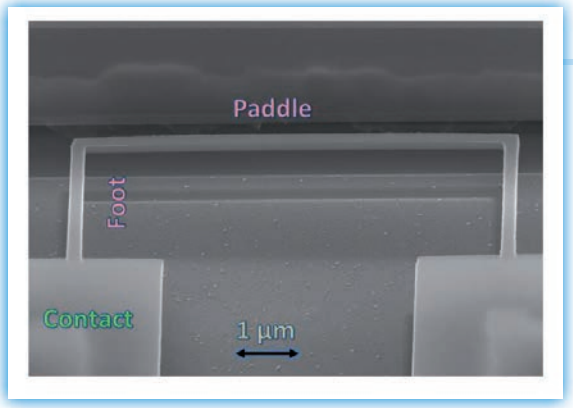

Fig. 1: Scanning Electron Microscope (SEM) image of a silicon NEMS sample of "goalpost" type. The 7 µm long "paddle" bar is 150 nm thick x 250 nm wide, and 30 nm of aluminum is evaporated on the top surface. It vibrates out-of-plane thanks to the electromagnetic excitation force (magnetomotive scheme).

While providing the proper phenomenological grounds for the understanding of experimental data, the model is far too simplistic and some theorists have challenged the existence of any TLSs at all. The key to a proper understanding seems to be in the coupling mechanism between individual Two Level Systems or any other possible entities responsible for the low-energy properties. Estimates for the typical length scale marking the crossover between correlated and truly independent Two Level States are about 1 µm. This is well within the NEMS fabrication range.

Dedicated NEMS resonator devices can be viewed as probes sensing the friction processes occurring in their constitutive materials. To date, only a few experiments on the mechanical friction at low temperature (down to 20 milliKelvin) in amorphous NEMSs, using only a few different amorphous materials, are available in the literature. The overall features among published data look qualitatively the same, but no quantitative consensus exists. Furthermore, NEMSs have displayed much worse mechanical quality factors than bulk structures, a fact that is not yet properly justified but is certainly linked to the TLS to TLS interaction length.

When the mechanical material of the NEMS is a dielectric (silicon, silicon dioxide, silicon nitride...), a conducting overlayer is usually added on the structure. This metal can be either normal or superconducting, but in either case it influences the friction mechanisms. This fact, which had been overlooked in the literature up to now, has been very clearly demonstrated by our group. We have shown that, by switching the aluminium metal from normal to superconducting using an external magnetic field as a "control-knob", the friction experienced by a silicon NEMS (the vibrational device shown in Fig. 1) is greatly reduced (see the linewidth data of Fig 2).

One explanation for the phenomenon is a renormalization of the interactions among Two Level Systems in our samples due to the nearby presence of the metal, in particular with its conduction electrons. The exact nature of these TLSs remains a puzzle (are they on the surface? within the aluminium?), but clearly we have demonstrated that the electronic degree of freedom of the NEMS has to play a role in the damping mechanism. This information should be a new key to help "crack" the long-standing mystery of the TLS nature of amorphous materials.

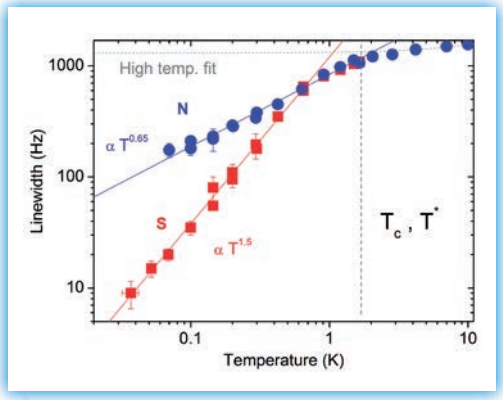

Fig. 2: An aluminium coated Si cantilever structure reaches quality factors $f/\Delta f$ of order one million around 20 mK, exceptional for a mechanical mode resonating around 10 MHz. N and S denote measurements with the Al in normal and superconducting states, while T (which happens to coincide with T_c, aluminium's critical temperature) marks the beginning of the damping decrease as T is reduced.*

CONTACTS

Eddy COLLIN
eddy.collin@neel.cnrs.fr
Olivier BOURGEOIS
olivier.bourgeois@neel.cnrs.fr

Ph.D student
Martial DEFOORT

FURTHER READING

Evidence for the Role of Normal-State Electrons in Nanoelectromechanical Damping Mechanisms at Very Low Temperatures
K. J. Lulla, M. Defoort, C. Blanc, O. Bourgeois and E. Collin
Phys. Rev. Lett. 110, 177206 (2013)

Tunable superconductivity in an array of metal dots decorating graphene

Nanoscale hybrid systems form an emerging family of devices whose particularity is to combine two materials of different nature (such as a molecule coupled to a metal, a semiconductor coupled to a superconductor, etc..). The heterogeneous association gives rise to synergies and provides new functionalities not present in either material alone. We focus here on a hybrid platform provided by graphene, an effectively two-dimensional, atomically-thin carbon sheet, decorated on its top surface with an array of tiny disks or nanoparticles of a superconducting metal such as tin or lead. This kind of device provides an experimental platform for studying quantum phase transitions in 2-Dimensional superconductors.

Superconductivity does not occur spontaneously in graphene (or, at least, no sign of intrinsic superconductivity has been detected so far). However, in our hybrid system (Fig. 1), because electronic charges in the graphene travel directly on its surface, they can easily "catch" some superconducting character by their coupling to superconducting dots adsorbed on top. That is, the correlations between pairs of electrons that produce superconductivity in the metal can "bleed" into the non-superconducting material over a given distance. This is an example of a fundamental phenomenon called the "proximity-effect".

It happens that graphene provides an ideal material for studying novel aspects of the proximity effect, this for three reasons: 1. The intrinsically low electronic density of graphene is not high enough to deplete the superconductivity in a system of tiny dots. 2. the exposed and relatively inert 2D electron gas on the graphene surface can be easily coupled to a 2D array of decorating dots ; there is efficient interfacial coupling and no strong potential barrier at the metal/graphene interface. 3. Last but not least, the strength of the resulting superconducting correlations in the graphene sheet can be tuned over a wide range by varying the "doping" (i.e. the density of graphene free-carrier charges) with a voltage *V* applied on a backgate electrode that generates a perpendicular electrostatic field (Fig. 1).

Thus, the graphene layer can play the role of a *variable resistance* 2D metal. Above a given threshold of the graphene's doping, the superconducting correlations from a superconducting dot can be transmitted far enough across the graphene to connect with the correlations emerging from neighbouring dots. This gives rise, by percolation, to a global superconducting state extending over the entire hybrid system. Thanks to the versatility of the hybrid platform, various parameters such as the order and symmetry of the metal dot array, its density, the nature of the materials and the structural quality of the underlying graphene can be studied over a large range.

High dot density can be achieved by a self-assembly method ("dewetting" of a thin film of metals such as Sn or Pb). This yields a two-dimensional, random array of metal-graphene-metal Josephson junctions. At the other extreme, by electron beam lithography we have got a metal density coverage as low as 3% for ordered triangular arrays of Sn dots with diameters a few hundred nm (see Fig.1), leading to a controllable superconducting state.

Interesting cases are obtained using disorder to modify the way superconductivity disappears in the hybrid system. Disorder in graphene can be produced in various ways. We first used slightly oxidized graphene where structural defects induce a regime of strong electronic localization at low temperatures, giving rise to a superconducting-to-insulating transition controllable by a gate voltage (see Fig. 2). More directly, in further experiments using low defect-density graphene, tuning the density of electrons with the backgate could effectively tune the degree of disorder more finely, just by changing the effective sheet resistance. When the coupling between dots becomes very small, quantum fluctuations in the superconducting phase of each island start to occur, giving rise to a metallic rather than an insulating state in this case. The system loses its superconductivity but residual superconducting correlations give the new metallic state some remarkable specific properties such as non-linearities.

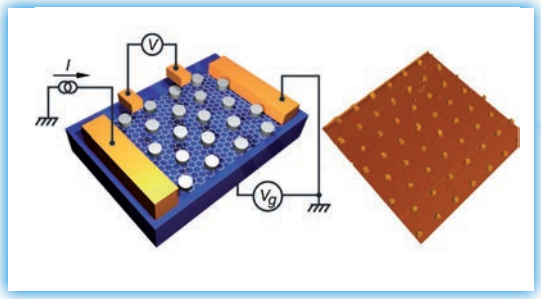

*Fig. 1. **At left** : Principle of a graphene transistor with tin disks (not to scale) decorating a graphene plane; the electrical properties are measured with four gold electrodes. **At right:** Atomic Force Microscope (AFM) micrograph of the central, active part of the device showing the triangular array of Sn dots.*

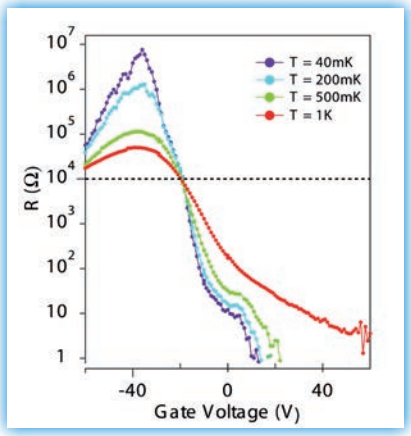

Fig. 2: Effect of varying the perpendicular electric field for various temperatures showing 7 orders of magnitude of resistance tuning at the lowest temperature. The large dynamic contribution of the conductance within the graphene layer enables us to observe a temperature-dependent transition from superconductor (at positive gate voltage V) to insulator at negative V.

In collaboration with theoreticians from Landau Institute, Moscow, we have demonstrated the existence of this "exotic" metallic phase which replaces the superconducting state at a critical level of disorder in the graphene. We could explore the quantum phase transition that exists between these two states. Our experimental results shed light on the process involved in suppression of superconductivity by disorder in a 2D system. The detailed behaviour of the quantum phase transition reveals a specific percolative regime and a universal resistivity predicted by the theory of percolation in 2D.

CONTACTS

Benjamin SACEPE
benjamin.sacepe@neel.cnrs.fr

Vincent BOUCHIAT
vincent.bouchiat@neel.cnrs.fr

Ph.D students
Adrien ALLAIN
Zheng HAN

FURTHER READING

Collapse of superconductivity in a hybrid tin-graphene Josephson junction array
Zheng Han, A. Allain, H. Arjmandi-Tash, K. Tikhonov, M. Feigel'man, B. Sacépé and V. Bouchiat
Nature Physics 10, 380 (2014).

Electrical control of the superconducting-to-insulating transition in graphene–metal hybrids
A. Allain, Zheng Han and V. Bouchiat
Nature Materials 11, 590, (2012).

Vortex creep in type II superconductors : when vortices cross walls

Perhaps the most striking property of superconductors, after the absence of electrical resistance, is their ability to expel a magnetic field. However, in the so-called "Type II" superconductors, the expulsion is incomplete : the magnetic field can penetrate to a certain extent into the superconductor forming quantized flux lines, called vortices. This "vortex matter" constitutes a very useful system to probe the physics of elastic systems in the presence of disorder, including the quantum creep of lines through a random pinning landscape.

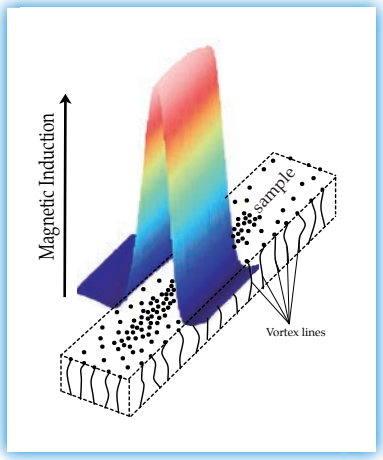

Fig.1: Profile of remnant magnetic field B across the Fe(Se,Te) sample, measured by scanning a miniature Hall probe sensor over the sample surface. The wavy lines (and dots on the surface) represent pinned vortices traversing the sample.

Vortices are field lines spreading through the sample. They are constituted of a non-superconducting core surrounded by permanent electric currents. When the magnetic field applied to a Type II superconductor is increased progressively, vortices form at the edges of the sample and penetrate laterally into it, finally reaching the sample's centre for high enough magnetic fields. The vortices are then expected to move back out of the sample as the field is reduced back to zero. However, some of them remain trapped inside the sample, as their non-superconducting core gets pinned by defects naturally present in all samples. A remnant magnetic field B then remains present even for zero applied field.

Since the magnetic flux carried by vortices is quantized, *B* is directly proportional to the vortex density and is hence much larger in the centre of the sample than at its periphery due to the larger number of vortices remaining pinned in the centre of the sample, see Fig.1. The corresponding magnetic field distribution is then characteristic of this out-of-equilibrium vortex state (called the "Bean state"), which can be measured by scanning a miniature Hall probe over the sample surface.

This flux distribution is however only metastable, and the vortices try to creep towards the sample edges to disappear from the sample. At finite temperature, they can jump over the barriers constituted by the pinning potential but this so-called thermal creep is expected to vanish when the thermal energy (k_BT) drops well below the pinning energy (U_p). However, vortices can also *pass through the (barrier) walls* (see Fig.2(a)), even at vanishing temperature.

The creep rate can be quantified by measuring the decay of the remnant magnetic field *B* at the centre of the sample. In the case of thermal creep, the decay rate S is expected to decrease with temperature as k_BT/U_p whereas, for quantum creep, *S* would remain finite down to zero temperature, being of the order of h/U_pt_c, where t_c is the time spent by the vortex under the barrier. This time scale is inversely proportional to the size of the creeping object i.e. in our case the vortex radius *R*, which is given by the coherence length. This *quantum* creep is similar to the quantum tunnelling of a single particle through any energy barrier but now concerns a vortex line (of radius *R*) spreading all the way through the sample.

So quantum creep is expected to be observed in systems where this radius (i.e. the coherence length) is particularly small. Iron Selenium Telluride belongs to the family of the iron-based superconductors discovered in 2009. This family has attracted much interest due to the presence of a magnetic element (Fe) and because the superconducting critical temperature can be as high as 55K (bettered only by the cuprates family). Our previous study of the *H-T* phase diagram has shown that the superconducting coherence length is indeed very small (~ 0.3 nm) in Fe(S,Te) which is therefore a very good candidate to look for quantum creep in vortex matter.

Using a Helium 3 cryostat built by the NEEL Institute's cryogenics service, we have been able to measure the relaxation rate *S* down to 0.3 K, see Fig. 2(b). We found that *S* remains finite down to the lowest temperatures (with *S*(0) ~2%). This shows clearly that quantum creeping is the dominant relaxation mechanism at low temperature and that the vortex lines can, indeed, pass through the pinning-potential walls to reach the sample edges, and thus disappear.

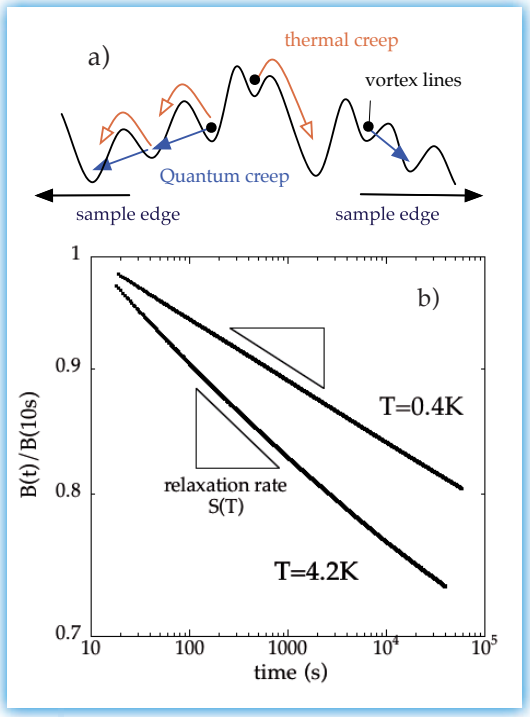

Fig. 2 (a): Vortex pinning potential. Vortex creep can be either thermally activated or due to quantum tunnelling through the barriers. (b): Decay of magnetic field (measured at sample centre) showing that creep remains present down to the lowest temperatures.

CONTACT

Thierry KLEIN
thierry.klein@neel.cnrs.fr

Ph.D student
Hadrien GRASLAND

FURTHER READING

Vortex creep down to 0.3 K in superconducting Fe(Te,Se) single crystals
T. Klein, H. Grasland, H. Cercellier, P. Toulemonde, and C. Marcenat
Phys. Rev. B 89, 014514 (2014)

Thermodynamic phase diagram of Fe($Se_{0.5}Te_{0.5}$) single crystals in fields up to 28 tesla
T. Klein, D. Braithwaite, A. Demuer, W. Knafo, G.Lapertot, C. Marcenat, P. Rodière, I. Sheikin, P. Strobel, A. Sulpice, and P. Toulemonde,
Phys. Rev. B, 82,184506 (2010)

Fibered nano-optical tweezers for micro- and nano-particle trapping

Optical "tweezers" are a means by which a small particle can be held stably in the electromagnetic field of a light beam. They have been a well established tool for non-invasive manipulation of very small objects in biology, chemistry, and soft-matter physics. In this context we are developing novel tweezers based on two optical-fibre nano-tips. Compared to standard optical tweezers based on focusing of a strong laser beam, our approach is more versatile and, especially, better adapted for trapping of nanoparticles.

The principle of optical tweezers (*fr."pinces optiques"*) can be understood by considering the optical forces affecting a small particle in a light field. The momentum exchange between the propagating light and the particle leads to a repulsive scattering force ("the pressure of light"). But the incoming light also induces an oscillating dipole inside the particle. This dipole feels a force pulling it up the gradient of the beam's intensity towards the maximum. Production of a strong gradient of intensity of the light is thus necessary for stable trapping. In the classical optical tweezers technique, first realized in 1986, a laser beam is focussed by a high numerical aperture microscope objective to obtain this strong light gradient in the axial direction.

Trapping of nanoparticles requires even stronger field gradients since optical forces scale with particle volume and as Brownian movement becomes more significant. Thus, near-field optical tweezers, utilizing a concentrating optical-fibre light source, and more specifically plasmonic tweezers, have been developed. In the case of fibered optical tweezers the light is tightly enough concentrated at the apex of the fibre tip that there is an intensity gradient steep enough to trap dielectric particles. However, as soon as we move even a little way from the fibre tip, scattering dominates and the particle is pushed away. The use of two fibre tips facing each other can overcome this limitation.

Fibre-based traps can work with samples that are inaccessible to the high-power microscope required for conventional optical traps. They can be used anywhere one can fit a mechanical probe. Today's micromanipulators can position the tip of a fibre with sub-nanometre accuracy, over a range of centimetres, combining the benefits of optical trapping with those of mechanical manipulation.

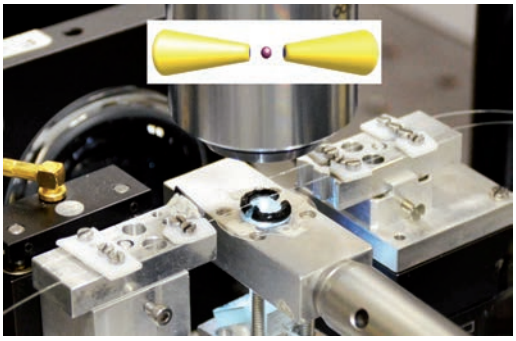

***Fig. 1**: Photo of our fibre nano-tip optical tweezers apparatus. (Inset drawing : fibre tweezers trapping a microsphere.)*

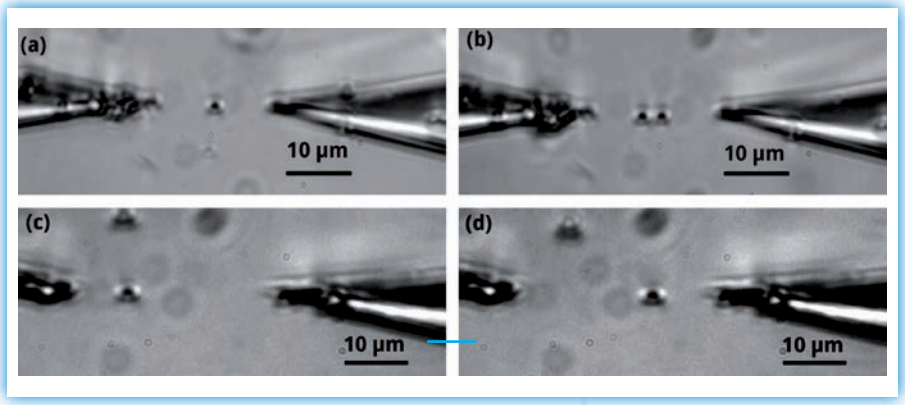

***Fig. 2**: Trapping of (a) one and (b) two micron-sized dielectric spheres using our dual fibre nano-tip optical tweezers. Images (c) and (d) show control of position of a single particle by modifying the relative light intensities in the two fibre tips.*

In this context we are developing a novel approach combining the advantages of fibered optical tweezers and plasmonic tweezers. Our "Fibred Plasmonic Nano-Tweezers" is based on an adjustable plasmonic cavity consisting of two nanometre-sized metalized optical fibre tips. The optical properties of these tweezers can be modified in real-time by controlling the tip-to-tip distance. The objective of this work is to trap and manipulate nanoparticles in order to study light-matter interactions at the nanometre scale.

As an important milestone, we have recently achieved stable and reproducible trapping of micro-particles and nano-particles using two bare (not yet metalized) optical fiber tips with tip-to-tip distances up to 28 µm and optical powers as low as 2.8 mW. The particle position along the optical axis can be controlled by varying the relative optical intensity injected into each fibre tip. Moreover, two or even more particles can be trapped for a few minutes. The effective potential of the optical tweezers can be calculated from trapping videos using three independent theoretical models. This showed that the trapping potential was harmonic with a trapping stiffness up to 35 pN $\mu m^{-1} W^{-1}$, well above the thermal energy of the trapped particles.

The results obtained are promising for projected trapping experiments for dielectric particles below 100 nm size. Metalized fibre tips of the type used in Nearfield Scanning Optical Microscopy (NSOM) can concentrate light into a spot only tens of nanometres across, creating an intensity gradient much higher than that available with a high-NA lens. This should prove very useful for trapping nanoparticles or other strongly scattering objects, and our technique would be perfect for characterizing such systems.

CONTACT

Jochen FICK
jochen.fick@neel.cnrs.fr

Ph.D student
Jean-Baptiste DECOMBE

FURTHER READING

Single and dual fiber nano-tip optical tweezers: trapping and analysis
J.-B. Decombe, S. Huant, J. Fick
Optics Express 21, 30521 (2013)

Unravelling structure and magnetism in strongly correlated systems

Doped $LaMnO_3$ compounds are a playground for the study of strong electronic correlations. Their remarkable properties under external magnetic field, such as the giant magneto-resistance in use in magnetic devices, is due to an intricate interplay between lattice, orbital and spin degrees of freedom. In this work we succeeded in decoupling the lattice and magnetic degrees of freedom leading to a new perspective on the fundamental processes that are in competition in these materials.

In $LaMnO_3$ (Lanthanum Manganite), the magnetic Mn atoms are in the charge state Mn^{3+}. This ion has four electrons in the 3d shell, with their spins parallel. The system spontaneously relaxes energy by distorting the cage containing the manganese (an octahedron of six oxygen atoms), splitting the highest occupied 3d orbital (the e_g energy level) by a mechanism called the "Jahn-Teller effect". This results in a cooperative Jahn-Teller distortion, i.e. a periodic, 3-Dimensional arrangement of distorted cages (see Fig. 1(a)) with associated orbital and magnetic orderings.

The underlying ordering of the atomic orbitals defines magnetic exchange pathways which give an overall antiferromagnetic structure (Fig. 1(b)). In the *ab* plane of the crystal lattice all the Mn's are ferromagnetically coupled: the Mn spins are parallel to each other. But neighbouring planes are antiferromagnetically coupled along the *c* axis (*z* in Fig. 1(b)).

It is well known that removing one electron to convert $3d^4$ to $3d^3$ induces the emergence of ferromagnetism in $LaMnO_3$. This has usually been done by replacing trivalent La by a divalent cation; in compensation, some of the $3d^4$ Mn^{3+} ions convert to the $3d^3$ charge state Mn^{4+}. There is no Jahn-Teller effect for the electronic configuration $3d^3$ (the e_g electronic level is unoccupied). Also, Mn $3d^3$ has a much smaller radius than Mn $3d^4$. Consequently, the emergence of a three-dimensional ferromagnetic component has been attributed to local changes in the symmetry of the octahedral cages, affecting the orbital ordering and the magnetic exchange pathways.

In our study we have doped $LaMnO_3$ with chromium, replacing some of the Mn^{3+} by Cr^{3+}. The Cr^{3+} ions have the same $3d^3$ configuration as Mn^{4+} but their ionic radius is closer to that of Mn^{3+}. We have found that, where a Cr $3d^3$ atom replaces a Mn $3d^4$ atom, the magnetic pathways change but, surprisingly, the nearby structure of distorted cages does not change.

We first proved by element-selective magnetic spectroscopies that there are in fact two ferromagnetic components emerging from the Cr doping. We found one from the host $3d^4$ Mn atoms, and a second one from the added $3d^3$ Cr atoms, each of these moments being proportional to the macroscopic ferromagnetism. Second finding, supported by *ab initio* calculations of the X-Ray spectra (see below): these two ferromagnetic components, were found to be antiparallel. It appears therefore that this doping with $3d^3$ atoms relaxes some of the antiferromagnetic coupling between the *ab* planes, producing the small overall ferromagnetic component.

We investigated the symmetry of the Mn and Cr cages using X-ray absorption near-edge spectroscopy at synchrotron facilities in France and Brazil. Unexpectedly, the spectra at the Mn and Cr X-ray K-edge were nearly identical in shape. This proves that the local electronic structure and therefore the structure of the oxygen cages are the same around the $3d^4$ ion Mn^{3+} and around the dispersed $3d^3$ ions Cr^{3+}. There is no significant reduction in the distortion, even though the Cr^{3+}, with its $3d^3$ configuration, does not have 3d level splitting.

Thus, the weakening of the antiferromagnetic Mn^{3+}-Mn^{3+} *c*-axis exchange pathway is not due to a restoration of the cage symmetry around the $3d^3$ ion. These conclusions contradict the theoretical model previously proposed for the emergence of ferromagnetism in doped $LaMnO_3$ compounds. We suggest a simple magnetic scheme compatible with our experimental results in Fig. 1(c).

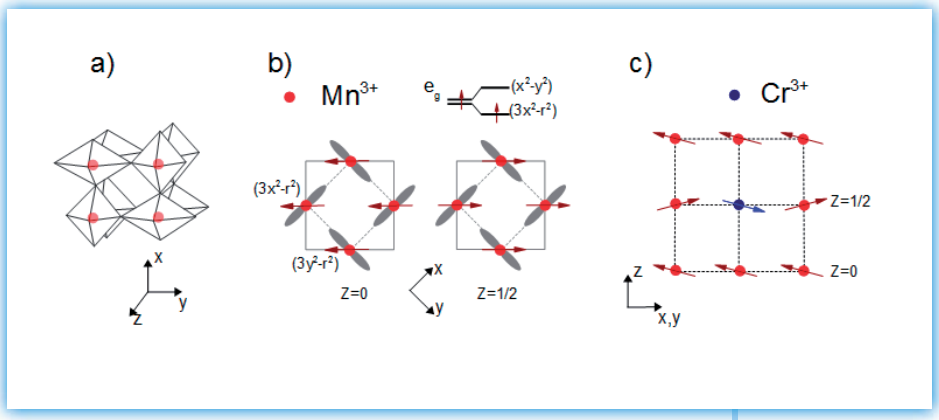

Fig. 1: (a) The 3D structural scheme of alternate, Jahn-Teller distorted MnO_6 cages in the orthorhombic crystal $LaMnO_3$. (b) Ordering of the e_g orbitals (represented in grey) and magnetic orderings (red arrows) in the ab plane for z =0 and z = c/2 (where z is the crystal c-axis). (c) Our proposed solution for the ferromagnetic ordering observed when an Mn is replaced by a Cr impurity.

CONTACTS

Aline RAMOS
aline.ramos@neel.cnrs.fr

Stephane GREINER
stephane.greiner@neel.cnrs.fr

FURTHER READING

Emergence of ferromagnetism and Jahn-Teller distortion in $LaMn_{1-x}Cr_xO_3$.
A.Y. Ramos, H.C.N. Tolentino, M.M. Soares, S. Grenier, O. Bunau, Y. Joly, F. Baudelet, F. Wilhelm, A. Rogalev, R.A. Souza, N.M. Souza-Neto, O. Proux, D. Testemale, and A. Caneiro.
Phys. Rev. B 87, 220404 (2013).

New mm-wave instrument ("NIKA") opens for astronomers

Millimetre-wave astronomy is an important tool for studying the cold and the primordial stages of our Universe. This branch of astronomy presents monumental challenges in detector science and technology. At the NEEL Institute, we have pioneered the development of the Lumped Element Kinetic Inductance Detectors (LEKIDs) technology. Our main driver was the construction of a new instrument for the Institut de Radioastronomie Millimétrique (IRAM). This instrument, called "NIKA" (acronym for New IRAM KID Array) was installed at the Sierra Nevada 30-metre radio-telescope in 2010 and is the most sensitive camera in the world using this innovative detection technology. Intense work on completing development of NIKA allowed its opening to the international astronomy community in February 2014.

Modern applications in millimetre and sub-millimetre astronomy require a large number of ultra-sensitive pixels, limited in sensitivity merely by photon counting statistics. This has been achieved in the past by using collections of a few tens of individual low temperature bolometers, cooled down to around 0.1 K (as used e.g. on the Planck satellite launched 2009). In the last few years, the challenge has been to develop monolithic filled arrays satisfying all the sensitivity requirements. But, on increasing the number of pixels, the practical issues associated with multiple electrical feed-throughs reaching into the cold focal plane of the telescope became a limiting factor. The Kinetic Inductance Detector (KID) concept, proposed by Caltech-JPL back in 2002, solves this puzzle in an elegant way.

KIDs are high quality-factor (Q = 10^4-10^6) superconducting resonators operated well below their critical temperature Tc. In a LEKID, they consist of a single patterned thin film of superconductor sensitive to the incoming radiation via the kinetic-inductance effect. The incoming photons break some of the electron pairs ("Cooper pairs") responsible for superconductivity, perturbing the complex impedance of the superconductor film and thus generating a measurable electrical signal. Many hundreds of KIDs can be multiplexed on a *single readout line* by adjusting their resonance frequencies to different values.

In 2010, our group designed and built an innovative, dual wavelength band, KID camera for the IRAM's 30 metre radiotelescope situated in Spain. Since then, in a highly competitive context, the group has driven the improvement of the NIKA instrument. The original name "Néel IRAM KID Arrays" has become the "New IRAM KID Arrays", reflecting the involvement since 2011 of a number of other groups in France (including LPSC, IPAG and IRAM in Grenoble, the IAS Orsay and CEA Saclay) and abroad (e.g. Cardiff University, IRAM Granada). As a result, this year, NIKA became the first KID-based instrument open to the general astronomical community. Compared to its direct competitor GISMO, based on the more standard bolometer technology and developed by NASA's Goddard Space Flight Center, NIKA has the distinct advantage of mapping the sky simultaneously at two wavelengths: 2.05mm and 1.25mm.

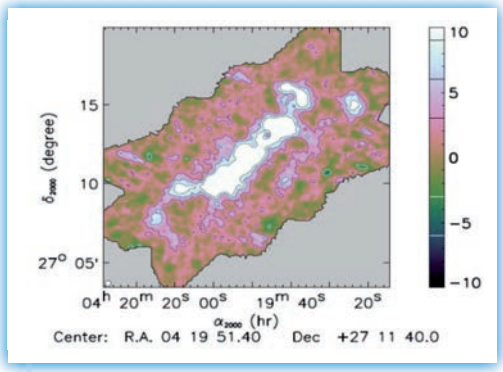

Fig. 1 : The Taurus interstellar dust filament mapped by NIKA at 150GHz (2.00 mm) during the first scientific run.

Fig. 2 : Part of the NIKA team at the Pico Veleta radio-telescope.

From left to right: M. Calvo, A. Catalano, A. Monfardini, J. Macias-Perez, N. Ponthieu.

In the period 14-28/02/2014, the NEEL Institute group leading the NIKA collaboration travelled to the IRAM 30-m telescope located at 2850-meters altitude on the Sierra Nevada, overlooking Granada. In winter the telescope is reached by cableway, followed by a snowcat journey or skiing. Once at the observatory, we worked together with colleagues of the NIKA collaboration in a challenging environment. On location remote from Grenoble, we ensured 24/24 hour support for all the NIKA hardware, ranging from the cryogenics to the detectors and readout electronics and data acquisition. With the astronomers and the IRAM-Spain staff, we checked the quality of the data in real time. We targeted and mapped with unprecedented sensitivity sources ranging from the planet Pluto to small-body disks around nearby stars, remote galaxy clusters, galactic interstellar dust filaments, gamma-ray bursts, etc. About 35% of the observations were done by the NIKA collaborators themselves; the remainder by external astronomers. The preliminary results indicate that NIKA has achieved a record sensitivity, being able to detect extremely faint sources with flux densities incident on the antenna of the order of 10^{-29} W/m²/Hz (10^{-3} "Jansky units").

Besides providing continuing support to the NIKA exploitation, our group at Institut NEEL is leading the NIKA2 project, based on the same key technologies, namely optical dilution cryostats and kinetic inductance detectors. NIKA2 will incorporate about 5,000 pixels, compared to 350 in NIKA. This will allow linear polarisation measurements at 1.25 mm wavelength, and a 10-fold increase of the mapping speed. The huge NIKA2 instrument is at present being assembled in Grenoble, in G2ELAB's big hall nicknamed "the cathedral". This ongoing work has involved a very large number of participants from the NEEL Institute's entire cryogenics and electronics groups.

CONTACTS

Alessandro MONFARDINI
alessandro.monfardini@neel.cnrs.fr
Alain BENOIT
Martino CALVO
Johannes GOUPY

Ph.D student
Antonio D'ABBADDO

FURTHER READING

Performance and calibration of the NIKA camera at the IRAM 30 m telescope
A. Catalano et al.
Astronomy and Astrophys. 569, A9 (2014)

Improved mm-wave photometry for kinetic inductance detectors
M. Calvo et al.
Astronomy and Astrophys. 511, L12 (2013)

At the interface between ab initio calculations and correlated models

Over the last few years, multiferroic compounds have become a hot subject of research. Indeed, the discovery of "colossal" magneto-electric effects in some of these compounds, i.e. a very large coupling between their electrical and magnetic properties, opens the possibility to control magnetic properties using an electric field and, in return, to control electric properties (polarisation, dielectric constant) by an applied magnetic field. Such systems may be fitted for applications in spintronics, for instance for new type of memories, captors, etc.. Thus, one of the challenges is to be able to design new materials presenting large magneto-electric coupling at room temperature. For this purpose it is essential to understand and predict the microscopic mechanisms responsible for : first the existence, and second the amplitude of the magneto-electric coupling.

In response to these challenges, we have developed a combination of different theoretical approaches, integrating viewpoints as different as Landau theory (macroscopic description of phase transitions essentially using symmetry analysis) and quantum chemical *ab-initio* calculations. Experimentalists measure macroscopic quantities such as the dielectric and magneto-electric tensors, the polarization, the magnetic order etc., as a function of temperature or applied fields. In order to design new materials we need to relate these properties to the microscopic nature of the system, that is its chemical composition and crystallographic structure. For this purpose one needs to build a complete image of the *microscopic degrees of freedom* (electronic, magnetic, spin-lattice coupling, spin-orbit coupling etc...) that are responsible for the observed macroscopic properties. This is what we have done for one of the archetypal multiferroic compounds Yttrium Manganite $YMnO_3$. ("Multiferroics" are materials in which two kinds of "ferric" orders exist and, by extension, systems in which two types of orders are coupled; in this case antiferromagnetism and ferroelectricity).

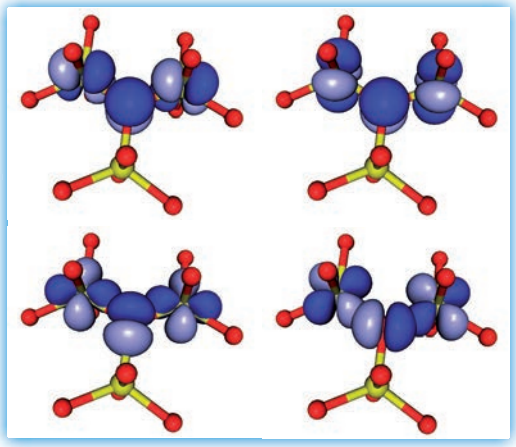

Fig. 1: Orbitals responsible for the magnetic coupling in $YMnO_3$ as obtained from a fragment ab initio calculation. Yellow atoms are Mn, red atoms are Oxygen. The two shades of blue correspond to the positive and negative parts of the O and Mn 3d orbitals. A spin-up electron in the right Mn 3d orbital can be exchanged with a spin-down electron in the left Mn 3d orbital, via complex electron hopping through the oxygen. For this exchange to take place, the O atom should possess bridging orbitals having large overlaps with the magnetic 3d orbitals of the two Mn atoms. Such orbitals are pictured here for each pair of magnetic Mn orbitals.

In a first step, using symmetry analysis of both the global (structural and magnetic) and local (second harmonic generation) experimental information, we were able to derive a Landau description of the magnetoelectric coupling explaining all the experimental data. This description involves four, coupled, order parameters and shows that the magnetic order does not belong to the totally symmetric irreducible representation of its group (a quite rare case). We also showed that the long searched-for switch of the sign of the electric polarization under a magnetic field is symmetry-forbidden and that only the amplitude of the polarization can be controlled in such a way.

In a second step we related the macroscopic properties to the microscopic degrees of freedom. For this purpose we computed the evolution of the magnetic coupling integrals as a function of an applied electric field, using *ab initio* calculations. "Ab initio" means solving in the most exact manner possible the Schrödinger equation for a few pertinent fragments of the real compound (Fig. 1). This point is the technical bottle neck since one cannot use mean-field type techniques for such strongly correlated systems. However, once solved and the (quasi)-exact local information being known, we derived an effective (simple) correlated-spin model mimicking these pieces of information, from which we were able to compute the macroscopic magneto-electric tensor. Our methodology (see schema) allowed us to relate the *macroscopic* measured tensor to the *microscopic* magnetic model and to the contribution of *each magnetic orbital*. This was possible because the quantum chemical calculation provides a full, detailed picture of the local *n*-electron wave-functions responsible for the magnetic couplings, as a function of the chemical composition and the atomic positions.

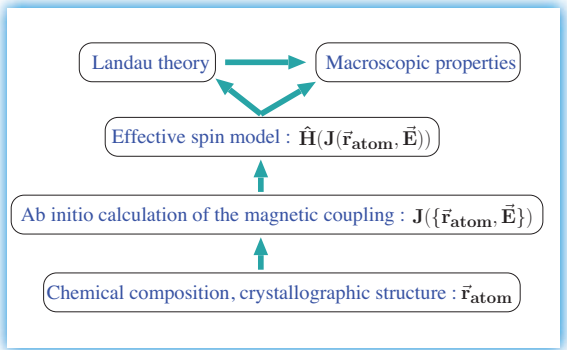

Such a method thus allows one to determine the role and amplitude of the possible mechanisms responsible for the magneto-electric coupling, such as for instance the so-called (inverse) Dzyaloshinskii–Moriya interaction (which we found could be ruled out for $YMnO_3$), the orbital or charge ordering (also ruled out for $YMnO_3$) and the exchange striction, which is the mechanism at work in $YMnO_3$.

CONTACT

Marie-Bernadette LEPETIT
marie-bernadette.lepetit@neel.cnrs.fr

Ph.D student
Julien VARIGNON

FURTHER READING

An ab initio study of magneto-electric coupling of $YMnO_3$
J. Varignon, S. Petit, A. Gellé and M-B. Lepetit
J. Phys.: Condens. Matter 25, 496004 (2013)

Analysis of the multiferroicity in the hexagonal manganite $YMnO_3$
K. Singh, M-B. Lepetit, C. Simon, N. Bellido, S. Pailhès, J. Varignon and A. de Muer
J. Phys.: Condens. Matter 25, 416002 (2013)

Mesoscopic spin glasses

A glass is arguably the strangest phase of ordinary matter; it is neither a liquid nor a crystalline solid, but it has aspects of both. One of the simplest glass structures is the spin-glass. We have started a project aiming at elucidating the physics governing these strange systems using tools coming from another domain of condensed matter physics, namely mesoscopic physics. This problem illustrates how a given field of research can benefit from other fields developed separately, or even from fundamental mathematics.

In the late 60s, a new phase of matter, called a "spin glass", was discovered in non-magnetic compounds doped with magnetic impurities. The problem is actually very simple: because the impurities are randomly distributed, their mutual magnetic interactions (the "RKKY interactions") will also have a random distribution, especially because the sign of these interactions depends on the distance between impurities. So interactions between two impurities will force the impurities' spins to be aligned parallel or anti-parallel randomly, depending on the distance between them. It is easy to understand that it will be impossible to satisfy all the constraints of the system: it is said to be "frustrated", the system cannot choose between multiple possible spin configurations. The nature of the ground state of a spin glass is still mysterious and a heavily debated subject; the most intriguing property is that this state consists of a large (possibly infinite) number of degenerate states. This can be described by a very fancy mathematical formalism: by defining the "distance" between two states by the number of spins which are flipped between the two configurations, it can be shown that the phase space is "ultrametric". This is one striking example of the intimate relation between Nature and a fundamental mathematical concept such as topology.

However, so far, no experiment had been able to probe the ground state of a spin glass and exhibit the ultrametric nature of its phase space. The problem is that almost all the experiments have concerned magnetization measurements, which yield only an *average* quantity over the whole sample. We need to probe the *microscopic* configuration of the spins. Here, the techniques of mesoscopic physics, a field that studies quantum coherent conductors, can help. Since the 1990's and the emergence of this domain, it has been known that electronic transport in a quantum system is directly related to the transmission of the quantum waves associated with the conduction electrons. Diffusion of electrons over a magnetic impurity leads to a dephasing, and thus modifies the transmission; the conductance thus reflects exactly the spin configuration of the spin glass.

This is the subject of our experiment. We measure the conductance of mesoscopic-scale spin glasses (small wires of a conducting metal containing some magnetic impurities) at very low temperature, as a function of an external parameter such as magnetic field. As can be seen in Fig. 1, the conductance exhibits oscillations as a function of a magnetic field. These fluctuations are not noise : they are the so-called "Universal Conductance Fluctuations" (UCF's). The fluctuations are resolved because there is only a relatively small number of channels of conduction in the mesoscopic sample. They are a true "magneto-fingerprint" of the sample; any change in the spin configuration will change this fingerprint. Such measurements are a powerful tool for probing the nature of the phase space of a spin glass.

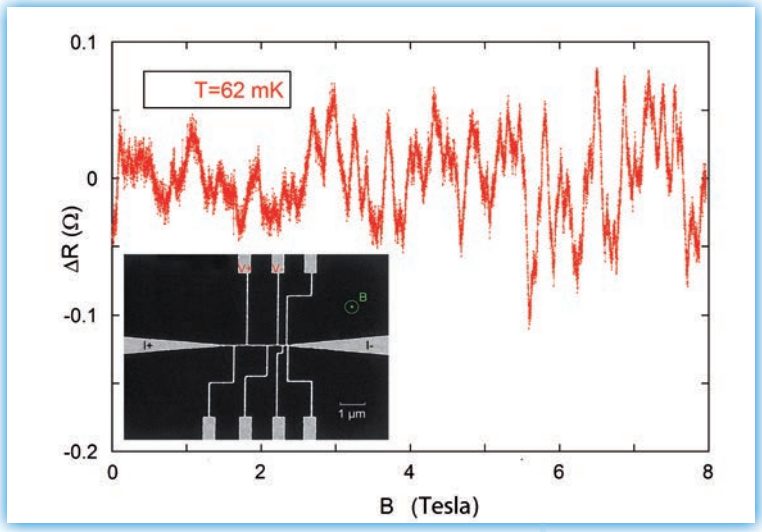

Fig. 1: Magneto-fingerprint of the spin glass Mn-doped silver measured at very low temperature (0.06 K). The conductance of the short (≈1 micron) wire section shown in the inset image fluctuates with magnetic field B. The fluctuations are perfectly reproducible and their precise shape corresponds to the configuration of the spins in the sample.

In recent work, we have made the first step in this direction by showing that these UCF's can tell us the number of free spins, i.e. spins that are not frozen, in the sample. This is actually a very old and recurrent question in the domain of spin glass physics: At the freezing temperature, do all the impurity spins freeze at the same time, as in a standard phase transition, or are things more complicated? We can answer this question because the Universal Conductance Fluctuations provide a direct measurement of the phase-coherence time of the electrons, which is directly related to the number of free spins (because spin-flips cause loss of coherence of the electrons).

We found that the glassy transition is more complicated than usual phase transitions: The transition does not appear at a precise temperature, but spreads over an extremely large temperature range. At the freezing temperature T (typically 700 mK in our case), only a fraction of the spins actually start to freeze, and freezing of the other spins occurs progressively down to very low temperature. At temperature T/10, almost 10% of the spins are still free.

This observation sheds new light on this very peculiar phase transition, and may help explain other strange experimental facts observed only for spin glasses. Finally, we have also found that spin glass systems are surprisingly robust against a very strong magnetic field : after a magnetic field cycling of magnitude several Teslas, the system ends up in *exactly the same microscopic spin configuration*. This unexpected observation could be related to the existence, in the glassy phase, of spin configurations much more "rigid" than the others, configurations the system will fall into after applying the strong magnetic field.

Mesoscopic physics is now a mature science, and it may lead to new dynamism in the field of the physics of complex systems. Our experiments give only a foretaste of the possibilities of this approach.

CONTACT

Laurent SAMINADAYAR
laurent.saminadayar@neel.cnrs.fr

Ph.D students
Thibaut CAPRON
Guillaume FORESTIER

FURTHER READING

Remanence effects in the electrical resistivity of spin glasses
T. Capron, A. Perrat-Mabilon, C. Peaucelle, T. Meunier, D. Carpentier, L. P. Lévy, C. Bäuerle and L. Saminadayar
Europhys. Lett. 93, 27001 (2011)

Superconductivity Dome around a Quantum Critical Point

The interplay between ordered states and the superconductivity that develops when they are destabilized is central in the understanding of subjects as diverse as high temperature superconductors and quantum chromodynamics. In the case of the Heavy Fermion family of compounds, superconductivity develops in a region of the phase diagram enclosed by a dome-shaped boundary. Our measurements show that such "Domes" are not restricted to these antiferromagnetic compounds, but also appear in materials with totally different types of interactions. As a consequence, the theories claiming to explain superconductivity domes should be of universal character.

A quantum phase transition is a transition from an ordered to a disordered phase (e.g. from a antiferromagnetic to a paramagnetic phase) that is not driven by temperature but by an external parameter, such as pressure, at $T = 0$. Such transitions are unusual, as they are caused not by thermal fluctuations but by quantum fluctuations rooted in the Heisenberg Uncertainty Principle. A huge amount of work on this subject has been done in Heavy Fermion compounds (a class of Rare Earth metal alloys). Intriguingly, very often these compounds develop superconductivity below a dome in their phase diagram, centred at the "Quantum Critical Point" (QCP) i.e. the point where their antiferromagnetic ordering disappears. This suggests that Quantum Critical Points play an important role in promoting superconductivity, e.g. by increasing the quasiparticle interaction.

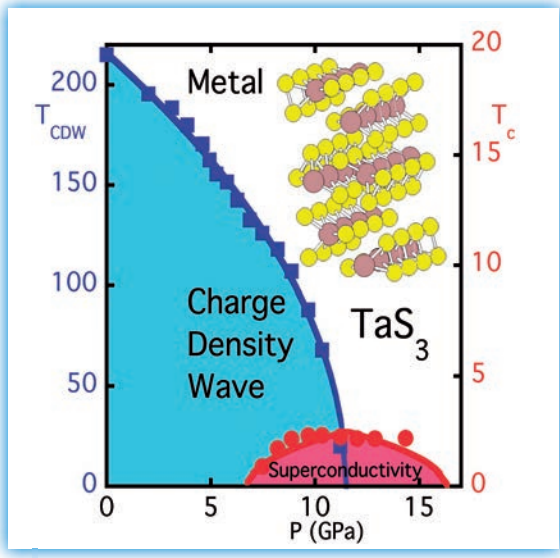

Fig. 1 : Temperature-pressure phase diagram for o-TaS_3. The critical temperature T_{CDW} for the Charge Density Wave phase (left hand y-axis) follows a mean-field power law. The superconductivity critical temperature T_c (right hand y-axis) follows a dome-shaped boundary surrounding the Quantum Critical Point of the CDW phase transition at P_c =11.5 GPa; thus superconductivity coexists with CDWs in a region below P_c. (In the linear crystal structure shown, brown and yellow spheres correspond, respectively, to the Ta and S atoms of o-TaS_3.)

The physics of Quantum Critical Points has also been invoked to explain the high-T_c superconductivity in copper-based high temperature superconductors even though a clear ordering under the superconducting Dome has not yet been identified. One possibility is that the important order in cuprates is of the Charge Density Wave (CDW) type (a type of 1 or 2 Dimensional ordering of the electronic density). It is thus of great interest to find clear examples where superconductivity coexists with CDWs, to provide model systems to study this interplay.

Within this context, we have studied the metallic, linear-chain compound Tantalum Trisulphide (o-TaS_3), which develops into an insulating, Charge Density Wave phase at T_{CDW} =215 K. We have measured its electrical resistivity from 300 K down to 1 K over a wide range of pressures. These experiments have allowed us to analyze in detail its pressure-temperature QCP and to identify the coexistence of CDWs and superconductivity .

The data show the metal to insulator transition temperature T_{CDW} decreasing monotonically with pressure, and the appearance of a superconducting state at critical temperature Tc under high pressure. Fig. 1 shows the evolution of these two transition temperatures with increasing pressure (note the two very different scales for T_{CDW} and T_c). Unexpectedly, T_{CDW} follows a mean-field type power law in the whole pressure range. In contrast, the superconducting phase develops under a dome, as found in the very different Heavy Fermion compounds.

In the field of Heavy Fermion systems, much discussion has been developed about the Dome and whether the superconductivity is due to the existence of a Quantum Critical Point. One hypothesis is that the carriers would forestall the intense critical fluctuations of the QCP by reorganizing themselves into a new stable phase of matter, i.e., superconductivity. On the contrary, in our case of a Charge Density Wave compound, it is natural to expect the appearance of superconductivity as the CDW phase disappears, since both are due to a conventional electron-phonon interaction. What is totally unexpected is the observed, dome-shape of the superconducting phase boundary. This suggests that something not taken into account by existing theories is occurring.

A hint is given by the fact that T_{CDW} follows a power law with pressure, instead of the logarithmic law expected from the Bardeen-Cooper-Schrieffer (BCS) character of the CDW state. Near the Quantum Critical Point we are no longer in what can be called a "classical" BCS regime, but in a critical quantum regime, with different laws and special physics. Our experimental result stresses the fact that superconductivity "domes" are not restricted to Heavy Fermion systems, but also occur in entirely different materials. As a consequence, the laws governing the Domes are definitely very general, as should be the theories proposed to explain them.

CONTACT

Manuel NUNEZ-REGUEIRO
manolo.nunez-regueiro@neel.cnrs.fr

FURTHER READING

Quantum critical point and superconducting dome in the pressure phase diagram of o-TaS_3
M. Monteverde, J. Lorenzana, P. Monceau and M. Núñez-Regueiro
Phys. Rev. B 88, 180504 (2013)

Bloch-point Domain Walls in cylindrical magnetic nanowires

Current data storage technology relies on storing bits at a surface, using optics (blu-Ray DVDs), electric charges (flash memory) or magnetism (hard disk drives). Progress in storage capacity will soon face a halt, as the shrinking size of individual bits faces fundamental limits. In 2004 IBM proposed a concept for a three-dimensional (3D) magnetic data storage device to progress beyond these limits. Series of magnetic domain walls would act as bits, moved along vertical nanowires by using the well-established "spintronics" property of spin transfer: the spin polarization of conduction electrons is transferred to magnetization, putting the walls into motion. This proposal has stimulated intense research activity on domain wall motion along one-dimensional systems.

So far, physics studies and demonstrator devices have been based on flat strips made by lithography, relatively easy to fabricate and access. True 3D designs require alternative routes, such as chemically-produced bottom-up arrays, yielding cylindrical nanowires. Theory has predicted that such cylindrical nanowires should host a new type of domain wall, the "Bloch-point" domain wall. Its name stems from the predicted existence of a Bloch point at the centre of this wall, on the wire axis. A Bloch point is an elusive though long-predicted object in micromagnetism close to atomic dimensions, where the magnitude of the magnetization vector should vanish : ferromagnetic order would be lost locally around a point (Fig. 1).

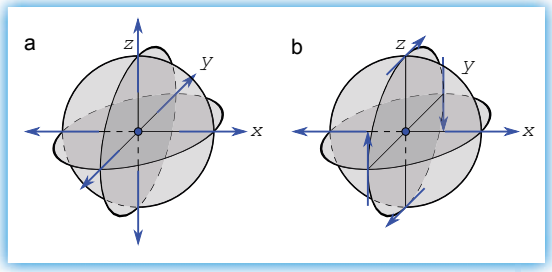

Fig. 1. Theory : Classical views for micromagnetic Bloch-points (the blue dot at the centre). The radial structure (a) associated with spherical symmetry (the so-called "hedgehog" structure) transforms into structure (b) (appropriate to cylindrical symmetry) by a π/2 rotation of magnetization around x, in the (yz) plane.

This property is imposed by the magnetization's needing to cover all directions in space around the domain wall, imposed by the boundary conditions at the scale of the entire object. These boundary conditions should provide topological protection to the wall, preventing its transformation into other types of magnetization texture. Simulations predict that this should allow reaching exceptionally high propagation speeds for such a wall, of the order of 1 km/s, under both magnetic field and spin-polarized current stimulation. Beyond the promise for disruptive technologies, this adds incentives for fundamental research on this new type of domain wall.

We prepared nanowires with diameters 50-100 nm by electroplating magnetic metals in self-organized anodized alumina templates. Here we considered permalloy ($Fe_{20}Ni_{80}$), a soft magnetic material suitable for domain wall motion. We released the wires by dissolution of the template, so as to study them lying on a surface.

Resolving the inner structure of such domain walls requires a bulk-sensitive magnetic microscopy, with 3D nature.

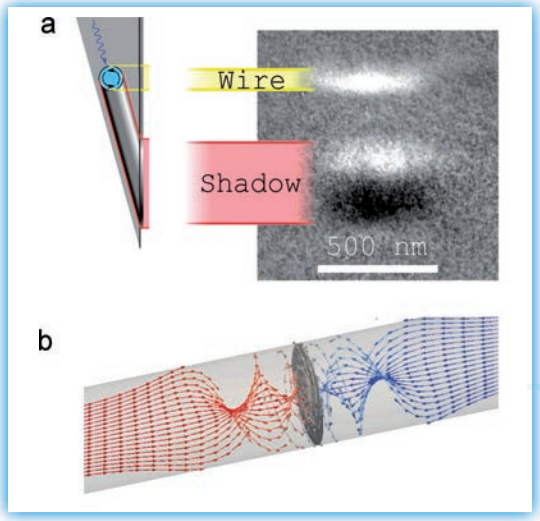

Fig. 2 : Experimental identification of the Bloch-point wall. (a) Principle of our X-Ray shadow microscopy experiment, along with the image of the shadow of a cylindrical permalloy nanowire showing the magnetic contrast at a Bloch-point domain wall. (b) Micromagnetic simulation of the streaming lines of magnetization inside the volume of the wire, corresponding to such an image.

We used high spatial resolution Photo-Emission Electron Microscopy combined with X-ray Magnetic Circular Dichroism (XMCD-PEEM), at the Elettra Synchrotron in Trieste. While this technique usually yields information at surfaces only, we also gathered volume information using a novel projection geometry which allowed us to measure the X-ray shadow behind the ultra-thin wire (Fig. 2(a)). The absorption of a polarised X-Ray as it goes through the wire diameter is sensitive to the direction of magnetization. We developed a dedicated micromagnetism computing code to analyze the data. This allowed us to identify the existence of the predicted Bloch-point domain wall in wires of diameter around 100nm and to propose the structure shown in Fig. 2(b). For smaller diameters we evidenced a so-called transverse wall, a more conventional type of domain wall, also predicted by theory for smaller diameters.

These results open the route to experiments to search for the predicted very high mobility of Bloch-point walls. In the framework of a European Union FP7-grant agreement (No.309589, M3d), we are tackling other fundamental issues responsible for bottlenecks in designing a working 3D memory. One of these issues is the proper design of diameter modulations along the wires, to localize domain walls in order to store bits. A technological requirement is to develop an error-tolerant scheme for shifting bits (domain walls) from one site to the next. Another issue concerns the magnetostatic interactions arising in a dense array of magnetic wires, because storage will require absence of "cross-talk" between adjacent wires. Overcoming this issue requires work to combine hardware solutions (design of the geometry of the array) and software solutions.

CONTACT

Olivier FRUCHART
olivier.fruchart@neel.cnrs.fr

Ph.D students
Sandrine DA-COL
Ségolène JAMET

FURTHER READING

Observation of Bloch-point domain walls in cylindrical magnetic nanowires
S. Da Col, S. Jamet, N. Rougemaille, A. Locatelli, T. O. Mentes, B. Santos Burgos, R. Afid, M. Darques, L. Cagnon, J.C. Toussaint and O. Fruchart
Phys. Rev. B 89, 180405 (2014)

Reduction of magnetostatic interactions in self-organized arrays of nickel nanowires using atomic layer deposition
S. Da Col, M. Darques, O. Fruchart and L. Cagnon
Appl. Phys. Lett. 98, 112501 (2011)

Project Website
Materials for a magnetic memory in three dimensions
http://mem3d.eu/

Evaporation of helium in a porous material

Porous materials are thirsty materials. Fluids whose liquid phase wets their substrate condense in porous materials at pressures smaller than the saturated vapour pressure, pressures where the bulk stable phase would be gaseous. For water, examples in everyday life range from the silica gels used as desiccants, to wood. Also, unlike in bulk conditions, the transition from gas to liquid shows strong hysteresis. Drying a porous material requires lowering the pressure well below the condensation pressure. Understanding the origin of the hysteresis, and the underlying evaporation mechanisms, is important for determining pore sizes distributions from the shape of the condensed mass vs pressure isotherms. In this work, we use a specific property of helium gas to demonstrate a crossover from a collective percolation evaporation mechanism to a local evaporation mechanism as the temperature is increased.

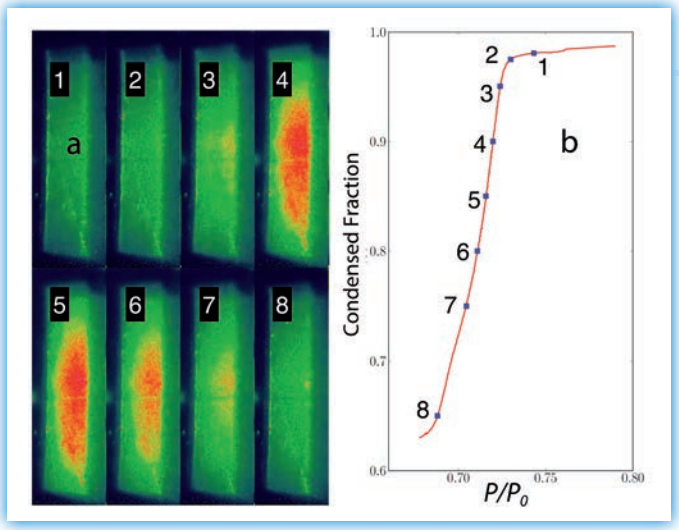

Fig. 1: Evaporation of helium in Vycor at 3 K. As pressure P is decreased below the saturated vapour pressure (P_0), the material empties. (a) Scattered-light images of a cross-section of the sample along the pressure isotherm of Fig. (b). The bright scattering signal is the signature of the collective nature of evaporation.

Condensation below the saturated vapour pressure is qualitatively explained by capillarity. In the same way as water rises in a thin straw, a fluid can condense in the narrow cylindrical channels of a porous material. The smaller the channel diameter, the lower the equilibrium pressure P_{eq} above which the liquid phase is stable.

Inversely, evaporation inside a channel open to the surface of the porous material can proceed at P_{eq} by recession of a liquid-gas meniscus inwards along the channel. However, in a disordered porous material, many of the pores are surrounded only by pores of smaller diameter. The bigger pores cannot empty at their equilibrium pressure as the neighbouring pores are filled with liquid, blocking the access to the vapour outside the sample. Evaporation must then proceed by one of two pathways, cavitation or percolation. Cavitation consists in the thermally activated local formation of a bubble. If cavitation cannot occur, and the pressure is decreased, all pores remain filled until potentially emptiable pores form a connected network (a percolation network) throughout the whole sample, at which point all these pores empty together.

It is expected theoretically that the evaporation mechanism should evolve from collective percolation to local cavitation as temperature increases, but experimental evidence for that has been scarce. In this work, we use light scattering to directly demonstrate the reality of this crossover.

Our porous material is a disk of Vycor, a porous silica glass with a topology similar to that of a sponge. Its interconnected pores are around 7 nm mean diameter and 30 nm in length, small enough for Vycor to be transparent to visible light. Our fluid is helium at temperatures below its critical point (5.2 K). Its extremely small refraction index (~1.02 at 3 K) allows us to use light scattering to probe the spatial distribution of the microscopic fluid. For other fluids of larger index, this would not be possible, as the large scattering would make the sample opaque, similar to a glass of milk.

Fig. 1(a) shows colour-coded images of the scattered light intensity in a cross-section of the disk. The sample is illuminated by a sheet of laser light propagating at a 45° angle with respect to the faces of the disk. Different images correspond to different stages of the evaporation process at a temperature of 3 K as the pressure *P* is lowered. This is to be compared with the remaining mass of liquid Helium inside the sample shown in Fig 1(b) as a function of pressure. The increased scattering brightness seen between points 2 and 7 implies that the fluid distribution is correlated over scales of distance much larger than the size of the pores, clear evidence for the expected collective effect. (At higher temperature, the scattering signal weakens and finally disappears, as local cavitation progressively sets in.)

Our result has practical consequences. The shape of condensation or desorption isotherms like those of Fig. 1(b) is widely used as a means to characterize pore-size distributions of porous materials, an important issue for many applications. This is based on the Barrett-Joyner-Halenda (BJH) theory, which assumes that pores empty independently at their size-dependent equilibrium pressure. For interconnected pores, this is at best an approximation. We are developing a model to establish criteria of approximate validity for the BJH method. Our experimental results will provide a benchmark for testing our approach.

CONTACT

Pierre-Etienne WOLF
pierre-etienne.wolf@neel.cnrs.fr

Ph.D student
Fabien BONNET

FURTHER READING

Light scattering study of collective effects during evaporation and condensation in a disordered porous material
F. Bonnet, M. Melich, L. Puech and P. E. Wolf
Europhys. Lett. 101, 16010 (2013)

Strain couples a nano-mechanical oscillator and a quantum emitter

In theory, the strangeness of quantum mechanics is not solely restricted to the microscopic world but applies equally to macroscopic objects. However, in practice, to get a macroscopic object to behave quantum mechanically requires an exquisite degree of control over the object and its environment. Recently, a new class of experimental devices has emerged, where such a thing is possible. These devices consist of a micro-mechanical oscillator in strong interaction with an externally controllable quantum degree of freedom. We have fabricated such a hybrid device by exploiting the simplest possible mediator to provide the coupling, namely the strain field in the material.

In spite of the tremendous success of quantum mechanics, the frontier between the quantum and the classical world is not included in the theory and still remains poorly defined. Owing to recent progress in nanotechnology, it is now possible to achieve well controlled interaction between the motion of a macroscopic object, specifically a mechanical oscillator of micron size, and a genuinely quantum degree of freedom such as a superconducting quantum bit or a semiconductor quantum dot. A mechanical oscillator can be cooled down into its quantum mechanical ground state, and a non-classical motion (a phonon number state) can then be excited via external control over a single quantum object coupled to it. Such a hybrid device must exhibit the largest possible coupling strength, and allow maximal control over the macroscopic quantum object.

In a collaboration between NEEL Institute teams and the nanofabrication facility at CEA-Grenoble, we have fabricated a new, fully monolithic, hybrid device, where the coupling mechanism is provided by the internal strain field generated by the motion of the mechanical oscillator. This device consists of a deformable "nanowire" (diameter in the 200 nm range) embedding a small number of semiconductor quantum dots (nanometre-scale inclusions of a semiconductor material). The quantum dots behave like artificial atoms that can emit light of frequency ω.

To begin with, a layer of Indium Arsenide (InAs) quantum dots is grown by Molecular Beam Epitaxy on a GaAs substrate and capped by an 18 µm thick GaAs layer. Nanowires are etched through this layer by a combination of electron beam lithography and reactive ion etching. The resulting wires looks like the one shown in Fig.1(a), with the quantum dot layer situated close to the bottom. This specific conical shape is designed to maximize optical access to the quantum dots (75% light collection efficiency has been demonstrated), which is a key property for realization of a useful, quantum opto-mechanical hybrid device.

The nanowire has a well-defined fundamental mode of mechanical vibration corresponding to the lateral flexion of the wire. Its resonance frequency $\Omega/2\pi$ is around 500kHz, with a quality factor of 3000 at T = 5 K. As shown in Figs 1(b) and (c), with the wire clamped by the substrate at its bottom end, the wire flexion generates a strain field within the material at the height of the quantum dot layer. The strain has maximal amplitude on the edge of the wire. Quantum dots situated in this area experience a periodic lattice deformation which modulates (i.e. causes a periodic shift $\delta\omega(t)$ of) their optical transition frequency.

We characterized the strength of this coupling by mechanical and optical spectroscopy of the hybrid device. The motion of the wire is monitored via the spatially sensitive reflection of a laser beam detected with a split photodiode. The frequency $\omega_0+\delta\omega(t)$ of the optical transition between a *single* quantum dot's ground and excited states (g) and (e) (see Fig.1) is monitored by photoluminescence stroboscopic measurements. We found that when the top of the wire moves by δx = 1 nm, the photoluminescence frequency shifts by $\hbar\delta\omega$ =200 µeV. Calibrating using the wire's thermal Brownian motion, we were able to infer a coupling strength of $g_0/2\pi$ =450 kHz.

This frequency can be understood as the spectral shift of the quantum dot induced by a single vibrational quantum in the nanowire. This coupling strength is very large as compared to state-of-the-art hybrid systems based on other strategies, and is even comparable with the mechanical frequency $\Omega/2\pi$. We are therefore close to the so-called strong-coupling regime where the spatial shift of the nanowire rest position caused by quantum dot excitation exceeds the nanowire's zero point fluctuation. In the future, the coupling strength could be still further enhanced by modifying the shape of the nanowire. This strain-based strategy is an important step towards the realization of an integrated, optically interfaced, external-field free, quantum hybrid system. It could be easily transferred to different materials such as the diamond nano-mechanical oscillator where Nitrogen-Vacancy colour centres constitute a quantum degree of freedom stable at room temperature.

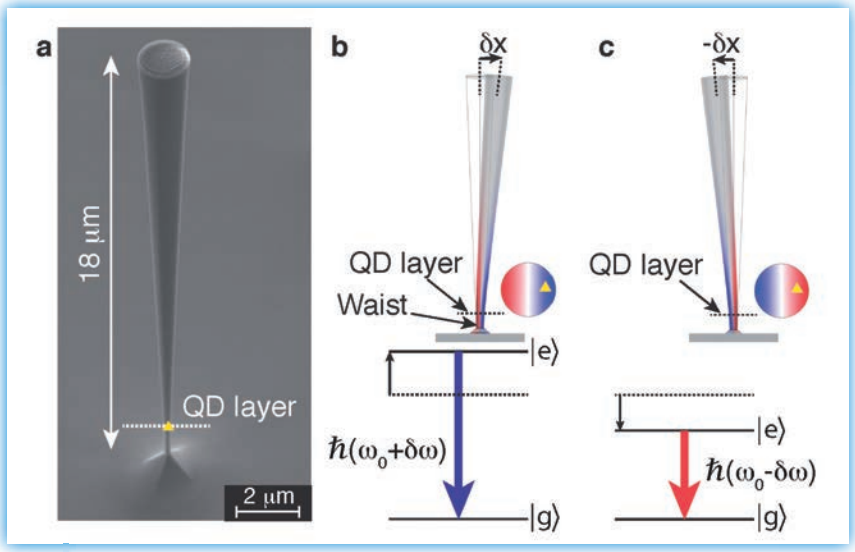

Fig. 1(a): Scanning Electronic Microscope image of the conical shaped GaAs nanowire embedding a layer of InAs Quantum Dots (QDs).
Fig. 1(b) and (c): When the top of the wire bends by +δx or -δx, the quantum dot depicted as a yellow triangle in the circular insets is under either compressive strain (blue) or tensile strain (red). The dot's optical transition energy ħω0 is either increased or decreased, by ħδω. Levels e and g represent the dot's excited and ground states, the dotted level represents the level e for δx=0.

CONTACTS

Jean-Philippe POIZAT
jean-philippe.poizat@neel.cnrs.fr
Olivier ARCIZET
Maxime RICHARD

Ph.D students
Inah YEO
Arnaud GLOPPE

FURTHER READING

Strain-mediated coupling in a quantum dot–mechanical oscillator hybrid system
I. Yeo, P-L. de Assis, A. Gloppe, E. Dupont-Ferrier, P. Verlot, N. S. Malik, E. Dupuy, J. Claudon, J-M. Gérard, A. Auffèves, G. Nogues, S. Seidelin, J-Ph. Poizat, O. Arcizet and M. Richard
Nature Nanotech. 9, 106 (2014).

Activation mechanism in the hydrogen storage material MgH_2

Hydrogen, produced by electrolysis of water, has huge potential as a sustainable energy carrier for storage of the "green" electricity produced by renewable sources. It can be used in fuel cells or even burnt directly in internal combustion engines. But a major obstacle to the expansion of hydrogen-based technology is the lack of compact and safe storage systems. For this purpose, metal hydrides, MH_x, are being intensively studied. They allow reversible loading and release of hydrogen according to the reaction: M + xH <—> MH_x. The hydrogen atoms are densely and securely packed in the metal lattice by chemical bonding.

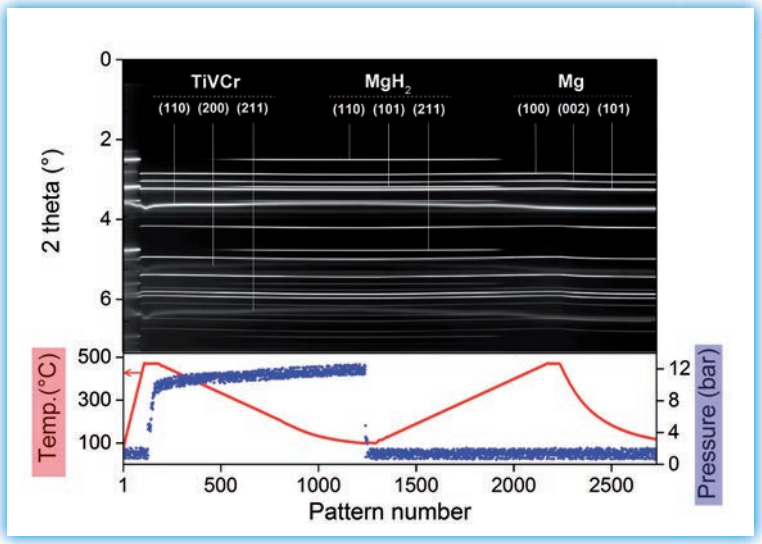

Fig. 1. At top : X-Ray diffraction intensities for a TiVCr-MgH_2 composite at wavelength λ= 0.1423Å, recorded as a function of time during an in situ experiment on the synchrotron beamline. Major Bragg peaks of the MgH_2, Mg and TiVCr phases are labelled. At bottom, the experimental conditions imposed : The hydrogen gas pressure (blue dots) during absorption (high pressure) and desorption (low pressure), and the sample temperature (red line).

Among the materials considered for hydrogen storage, magnesium hydride MgH_2 has great advantages. It can store 7.6 weight % hydrogen, and magnesium itself is abundant and non-toxic. Hydrogen is readily incorporated in magnesium powders under moderate gas pressure and released by lowering the pressure, dependent on temperature (desorption is endothermic so any accidental release of hydrogen is self-interrupting). The feasibility of MgH2 has already been demonstrated for application at the industrial scale by the French company McPhy Energy, created in 2008, which exploits techniques based on Néel Institute research.

The kinetics of hydrogen sorption in pure Mg is relatively slow but transition metal "additives", which are secondary phases intimately mixed into the hydrogen storage medium by ball milling (*fr: broyage*), have been found to be very efficient reaction accelerators. The additive's exact role is still unclear. The ball-milling process itself has beneficial effects. It produces dispersed, nanosized particles resulting in reduced hydrogen diffusion path lengths and increased coverage of the MgH_2 grains. In addition, two other explanations have been proposed: (1) a positive effect of microstrains induced by the mismatch of the thermo-mechanical properties, and (2) a "gateway" role of the transition elements where the oxygen-free Mg/transition metal interfaces, formed during ball-milling, are more permeable to hydrogen than oxidized surfaces, and therefore facilitate its sorption.

We have used X-Ray diffraction to understand the role of a transition metal alloy (titanium vanadium chromium TiVCr) in the sorption of hydrogen by magnesium. Our samples were composites consisting of an intimate mixture obtained by ball-milling MgH_2 and TiVCr alloy together. To measure the evolution of the crystal phases present during hydrogen absorption and desorption, apparatus was developed specially for an in-situ study on X-Ray beam line ID15 at the European Synchrotron Radiation Facility, Grenoble (T. Andrieux et al., J. Appl. Crystallogr. 2014). This apparatus can collect diffraction patterns at a high repetition rate: one pattern every 40 sec. The samples were contained in a sapphire capillary connected to a high-temperature, high pressure, gas loading system. The structural properties of the materials were investigated continuously while they underwent reaction under controlled temperature and hydrogen pressure (Fig. 1).

Analysis of the data provided identification and quantification of the different chemical phases present during hydrogen absorption and desorption reactions at temperatures 100-500 C. Lattice parameter values reflect volume changes resulting from hydrogen sorption. In particular, variations of the transition metal alloy's lattice parameters (adjusted for thermal expansion) showed that hydrogen was being inserted in the metal lattice of the additive to form a solid solution $TiVCrH_x$. While $TiVCrH_x$ shows a monotonic, progressive decrease in its volume as a function of dehydrogenation when studied as a pure material, it undergoes a sudden, anomalous volume change around 350 C in the composite mixture, coincident with the rapid decomposition of the MgH_2 fraction. Inversely, a similar behavior was observed upon hydrogenation of the composite.

These results provide clear evidence for a cooperative effect between the additive and the primary hydrogen storage medium MgH_2. We can assign the volume changes of the $TiVCrH_x$ phase to be directly related to hydrogen exchange between the additive and Mg or MgH_2 at the scale of the grains in the composite. These significant volume changes are obviously playing a role in modifying the mechanical strains at the Mg/additive interface within the composite.

In conclusion, the results elucidate the interaction between the additive and MgH_2 during reversible hydrogen loading and release. The present methods which were dedicated to MgH_2 composites could be used for the investigation and design of other efficient hydrogen storage systems, or more widely, to other applications in which composite materials are involved in solid-gas reactions. Our results could not have been obtained without performing the in-situ experiments at an intense synchrotron X-Ray source.

CONTACTS

Laetitia LAVERSENNE
laetitia.laversenne@neel.cnrs.fr
Salvatore MIRAGLIA
salvatore.miraglia@neel.cnrs.fr

FURTHER READING

In operando study of TiVCr additive in MgH_2 composites
L. Laversenne, J. Andrieux, D. Plante, L. Lyard, and S. Miraglia.
Int. J. Hydrogen Energy 38, 11937 (2013)

neel.cnrs.fr

Highlights 2014

Institut NÉEL
25, rue des Martyrs
B.P. 166
38042 Grenoble Cedex 9
neel.cnrs.fr

SYNTHESE ECA - 04 76 90 02 73 - Crédit photos : Institut NEEL